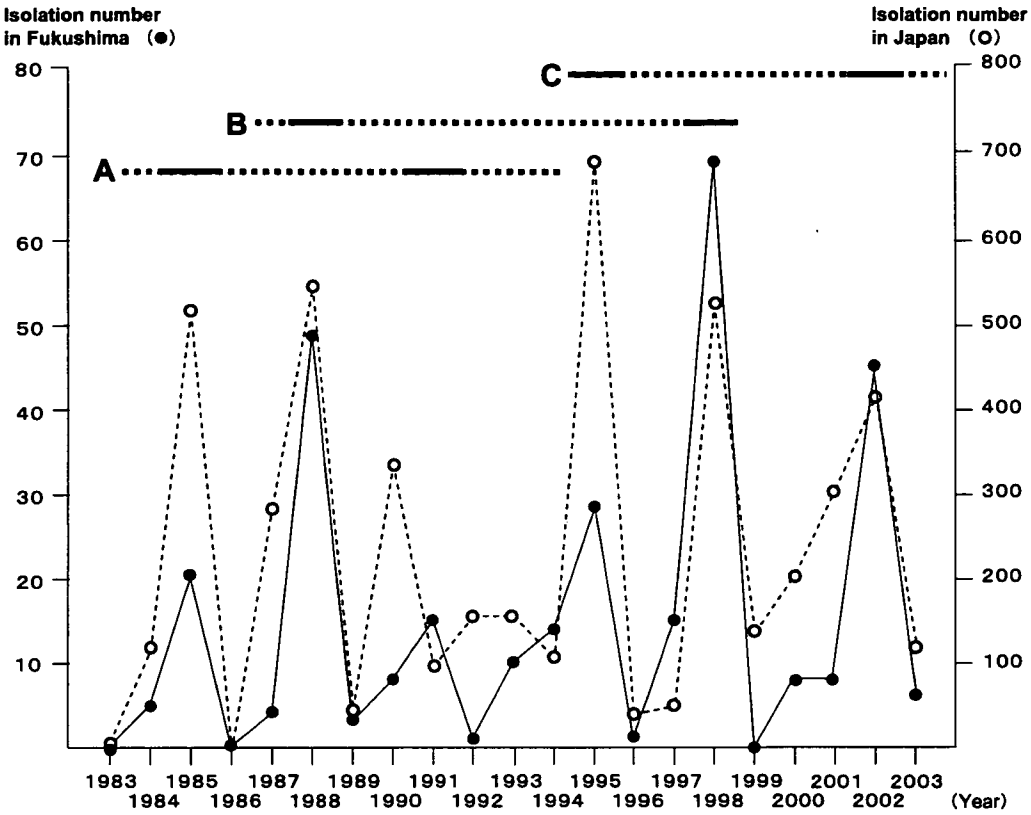

FIG. 1. Numbers of CV-A16 isolates in Fukushima Prefecture and in Japan between 1983 and 2003. Numbers of CV-A16 isolates in Fukushima (closed circles and solid line) and in Japan (open circles and broken line) are expressed, as reported to the Infectious Disease Surveillance Center in Japan by prefectural and municipal public health institutes through the Japanese infectious agents surveillance program. A, B, and C refer to genogroups designated based on phylogenetic analysis of the VP4 sequences of CV-A16 strains. Solid bars and broken bars indicate HFMD outbreaks and epidemic periods, respectively, due to corresponding genogroups.

cDNA reaction mixture was added to 45 μl of 1× *Taq* buffer containing 12.5 pmol of a forward primer, MD91 (nt 444 to 468, 5′-CCTCCGGCCCCTGAAT GCGGCTAAT-3′) and 2.5 U of *Taq* DNA polymerase (Roche Diagnostic Systems). Seminested PCR was performed using 5 μl of the PCR product with a pair of primers, EVP4 (nt 541 to 560, 5′-CTACTTTGGGTGTCCGTGTT-3′) and OL68-1. After initial denaturation at 94°C for 5 min, 40 cycles of amplification were performed by using the GeneAmp PCR System 9600 (PE-Applied Biosystems). Each cycle consisted of denaturation at 95°C for 30 s, primer annealing at 55°C for 30 s, and an extension reaction at 72°C for 1 min. The 40 amplification cycles were followed by a final extension at 72°C for 7 min. The first PCR primer pair allowed for amplification of 753 bp, and the seminested PCR primer pair allowed for amplification of 656 bp. The final PCR products encoded the 3′ one-third of the 5′ nontranslated region, the entire VP4, and the 5′ one-third of VP2 of each CV-A16 strain. The PCR products, including the entire VP4 sequences, were separated in 1% agarose gels and purified with a QIAquick gel extraction kit (QIAGEN). The nucleotide sequence was determined by using a 373A DNA autosequencer (PE-Applied Biosystems) with fluorescent dideoxy chain terminations (PE-Applied Biosystems) and EVP4 and OL68-1 primers.

Phylogenetic analysis based on the VP4 gene. The entire VP4 nucleotide sequences of the 129 strains isolated in Fukushima were determined and used for phylogeny-based analysis, along with those of 64 prototype enterovirus strains. We estimated the evolutionary distances using the Kimura two-parameter method (8) and constructed unrooted phylogenetic trees with the neighbor-joining method (14). Bootstrap analysis was performed by resampling the data sets 1,000 times. Bootstrap values greater than 70% were considered to be statistically significant for the grouping. The VP4 sequences of representative 54 CV-A16 strains isolated in Fukushima were also compared to those of 20 strains isolated in other areas of Japan, 29 strains in China, and 1 strain in the United Kingdom taken from international databases (GenBank) by using phylogenetic analysis.

PCR and phylogenetic analysis based on the VP1 gene. To confirm the relevance of genogrouping based on the VP4 region, we used the phylogeny-based classification methods using the VP1 sequences that were reported by Oberste et al. (12). Twenty-five CV-A16 strains isolated in Fukushima were randomly selected, and their VP1 regions were amplified using two sets of primer pairs, i.e., 055/VP3-011/2A and 055/VP3-009/2A. The VP1 sequences were determined and compared by using phylogenetic analysis with those of 28 strains isolated in China and 1 Taiwan strain taken from international databases.

RESULTS

Chronologic genetic diversity. Enterovirus surveillance data in the Fukushima Prefecture for the period from 1983 to 2003 indicate that peaks of CV-A16 isolations from HFMD occurred in 1985, 1988, 1991, 1995, 1998, and 2002. This epidemic pattern is very similar to that observed in Japanese national surveillance data (Fig. 1) (6). A total of 322 CV-A16 strains were isolated and identified during this period in the Fukushima Prefecture. A nested RT-PCR assay was performed for the detection of enteroviral genome sequences in 63 randomly selected samples collected from 1983 to 1999 and in the 69 samples collected from 2000 to 2003. A positive PCR result was obtained in 129 of 132 samples, and all detected enteroviruses were identified as CV-A16 using PCR-based analysis. Phylogenetic analysis of the VP4 sequences of 129 CV-A16 strains isolated in Fukushima demonstrated the existence of at

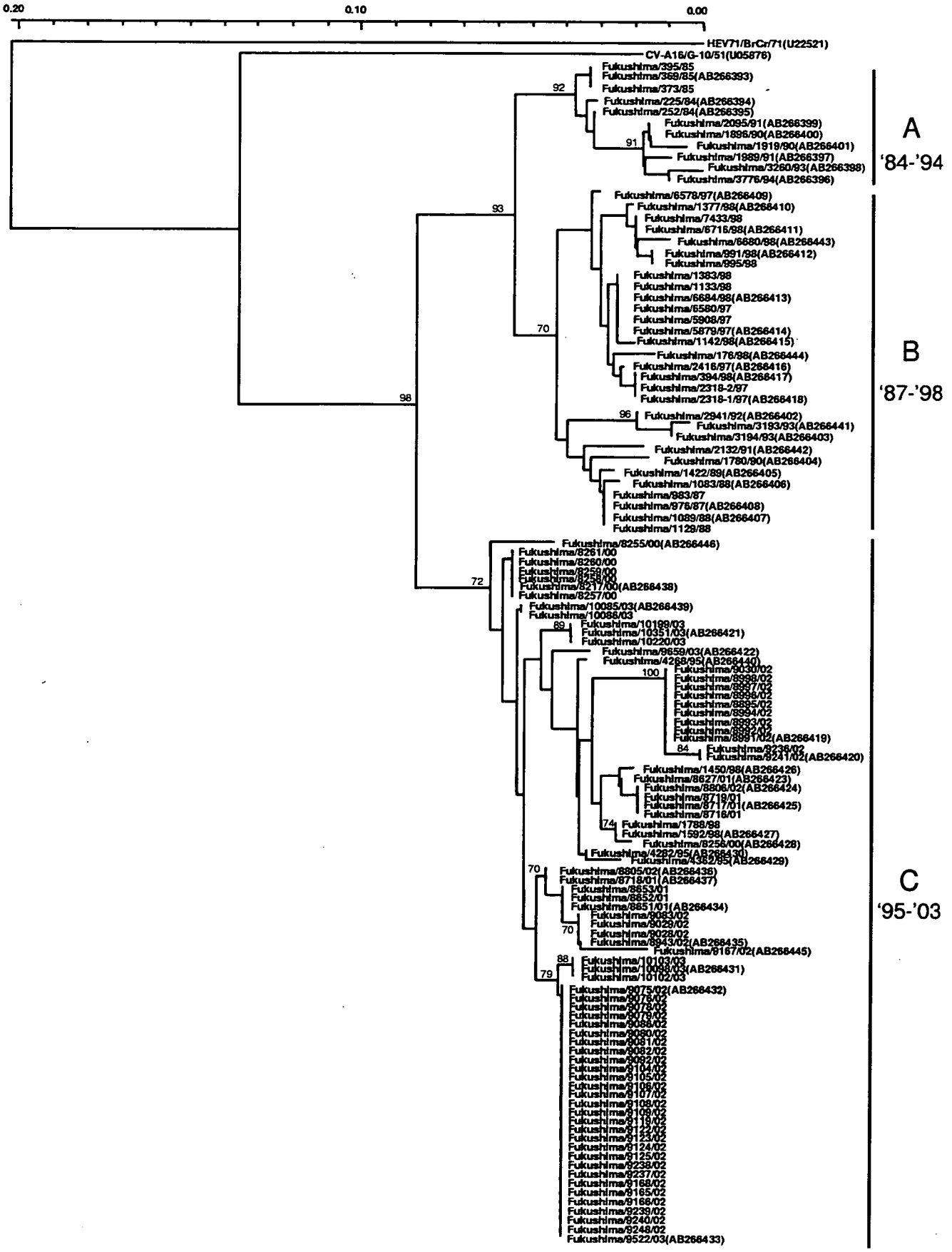
0.20
0.10
0.00
HEV71/BrCr/71(U22521)
CV-A16/G-10/51(U05876)
Fukushima/395/85
Fukushima/368/85(AB266393)
Fukushima/373/85
Fukushima/225/84(AB266394)
Fukushima/252/84(AB266395)
Fukushima/2095/91(AB266399)
Fukushima/1896/90(AB266400)
Fukushima/1919/90(AB266401)
Fukushima/1989/91(AB266397)
Fukushima/3260/93(AB266398)
Fukushima/3776/94(AB266396)
A
'84-'94
Fukushima/6578/97(AB266409)
Fukushima/1377/98(AB266410)
Fukushima/7433/98
Fukushima/6716/98(AB266411)
Fukushima/6680/98(AB266443)
Fukushima/991/98(AB266412)
Fukushima/995/98
Fukushima/1383/98
Fukushima/1133/98
Fukushima/6684/98(AB266413)
Fukushima/6580/97
Fukushima/5908/97
Fukushima/5879/97(AB266414)
Fukushima/1142/98(AB266415)
Fukushima/176/98(AB266444)
Fukushima/2416/97(AB266416)
Fukushima/394/98(AB266417)
Fukushima/2318-2/97
Fukushima/2318-1/97(AB266418)
Fukushima/2941/92(AB266402)
Fukushima/3193/93(AB266441)
Fukushima/3194/93(AB266403)
Fukushima/2132/91(AB266442)
Fukushima/1780/90(AB266404)
Fukushima/1422/89(AB266405)
Fukushima/1083/88(AB266406)
Fukushima/983/87
Fukushima/976/87(AB266408)
Fukushima/1089/88(AB266407)
Fukushima/1129/88
B
'87-'98
Fukushima/8255/00(AB266446)
Fukushima/8261/00
Fukushima/8260/00
Fukushima/8259/00
Fukushima/8258/00
Fukushima/8217/00(AB266438)
Fukushima/8257/00
Fukushima/10085/03(AB266439)
Fukushima/10086/03
Fukushima/10199/03
Fukushima/10351/03(AB266421)
Fukushima/10220/03
Fukushima/9659/03(AB266422)
Fukushima/4268/95(AB266440)
Fukushima/9030/02
Fukushima/8998/02
Fukushima/8997/02
Fukushima/8996/02
Fukushima/8995/02
Fukushima/8994/02
Fukushima/8993/02
Fukushima/8992/02
Fukushima/8991/02(AB266419)
Fukushima/9236/02
Fukushima/9241/02(AB266420)
Fukushima/1450/98(AB266426)
Fukushima/8627/01(AB266423)
Fukushima/8806/02(AB266424)
Fukushima/8719/01
Fukushima/8717/01(AB266425)
Fukushima/8716/01
Fukushima/1788/98
Fukushima/1592/98(AB266427)
Fukushima/8258/00(AB266428)
Fukushima/4282/95(AB266430)
Fukushima/4352/95(AB266429)
Fukushima/8805/02(AB266436)
Fukushima/8718/01(AB266437)
Fukushima/8853/01
Fukushima/8852/01
Fukushima/8851/01(AB266434)
Fukushima/9083/02
Fukushima/9029/02
Fukushima/9028/02
Fukushima/8943/02(AB266435)
Fukushima/9167/02(AB266445)
Fukushima/10103/03
Fukushima/10088/03(AB266431)
Fukushima/10102/03
Fukushima/9075/02(AB266432)
Fukushima/9076/02
Fukushima/9077/02
Fukushima/9078/02
Fukushima/9079/02
Fukushima/9088/02
Fukushima/9080/02
Fukushima/9081/02
Fukushima/9082/02
Fukushima/9092/02
Fukushima/9104/02
Fukushima/9105/02
Fukushima/9106/02
Fukushima/9107/02
Fukushima/9108/02
Fukushima/9109/02
Fukushima/9119/02
Fukushima/9122/02
Fukushima/9123/02
Fukushima/9124/02
Fukushima/9125/02
Fukushima/9238/02
Fukushima/9237/02
Fukushima/9168/02
Fukushima/9165/02
Fukushima/9166/02
Fukushima/9239/02
Fukushima/9240/02
Fukushima/9248/02
Fukushima/9522/03(AB266433)
C
'95-'03
92
91
93
70
98
96
72
89
100
84
74
70
70
88
79

least three genetically distinct groups (bootstrap value of >70%) relating to the epidemics that occurred from 1984 to 1994, from 1987 to 1998, and from 1995 to 2003 (Fig. 2). These three groups were designated genogroups A, B, and C, respectively. The outbreaks in 1985 and 1991 were due to genogroup A, those in 1988 and 1998 were due to genogroup B, and those in 1995 and 2002 were due to genogroup C (Fig. 1). All isolates in Fukushima since 2000 were of genogroup C. CV-A16 strains within a genogroup were slightly genetically divergent in several epidemics.

Geographic genetic relationship. VP4 sequences of representative 54 CV-A16 strains isolated in Fukushima were compared to those of 50 strains taken from international databases (GenBank), which included 20 strains isolated in Japan, 29 strains in China, and 1 United Kingdom strain. Genogroup A strains included 11 CV-A16 strains isolated in Fukushima from 1984 to 1994 and 1 strain isolated in another part of Japan in 1986. Genogroup B strains included 30 CV-A16 strains isolated in Fukushima from 1987 to 1998, 6 strains isolated in other parts of Japan from 1979 to 1998, and 3 strains isolated in Asia from 1999 to 2000. Genogroup C strains included 88 CV-A16 strains isolated in Fukushima from 1995 to 2003, 11 strains isolated in other parts of Japan from 1998 to 2002, 26 strains isolated in Asia from 1998 to 2003, and 1 United Kingdom strain in 1999. In general, each genogroup relating to the epidemics from 1984 to 1994, from 1987 to1998, or from 1995 to 2003 in Fukushima formed a single cluster with CV-A16 strains isolated during almost the same time period in other areas of Japan and in China (Fig. 3). Although the clustering seemed to be more closely related to the period of isolation rather than the area of isolation, the VP4 sequences of strains isolated in Japan were not identical to those isolated in China during the same time period. The GenBank accession numbers of the nucleotide sequences of 54 representative CV-A16 isolates in Fukushima are AB266393 to AB266446. These are indicated in parentheses in Fig. 3, as well as 50 additional strains taken from GenBank.

To clarify whether the genetic diversity occurred as clusters in the VP4 gene or scattered across the gene, the entire VP4 nucleotide sequences of all strains were aligned (Fig. 4). Common genetic diversities were observed in each genogroup. They did not form clusters but appeared randomly throughout the VP4 gene.

Phylogenetic analysis based on the VP1 gene. To confirm the relevance of genogrouping based on the VP4 region, bootstrap analysis was performed using VP1 sequences of 25 CV-A16 strains isolated in Fukushima and 29 strains isolated in other countries. The analysis based on the VP1 gene revealed three genetically distinct groups, and the grouping was completely identical to the results based on the VP4 gene (data not shown). Bootstrap values for the grouping of A, B, and C based on the VP1 gene were 97, 81, and 100%, respectively, and were higher than those based on the VP4 gene (90, 39, and 71%, respectively).

DISCUSSION

CV-A16 causes large outbreaks of HFMD worldwide. Enterovirus surveillance data in the Fukushima Prefecture for the period from 1983 to 2003 indicate that the annual proportion of CV-A16 isolates relative to total enterovirus isolates fluctuated widely, from 0% in 1983, 1986, and 1999 to 35.3% in 2002. Peaks of CV-A16 isolations from HFMD occurred in the years 1985, 1988, 1991, 1995, 1998, and 2002 (6). This epidemic pattern is very similar to that observed in the Japanese national surveillance data (Fig. 1) (6). These observations indicate that CV-A16 follows an epidemic mode of transmission, causing large outbreaks and then becoming quiescent for a period of a few years. Similar quiescence between outbreaks is observed in the meningitis epidemics caused by echovirus type 30. The quiescence is probably due to the development of population immunity that occurs during a high-infection-rate epidemic. The virus might cause only sporadic cases until a large cohort of nonimmune individuals has developed, often over a period of several years, setting the stage for another large epidemic (12).

Phylogeny-based classification using the VP4 sequence is useful for the identification of human enteroviruses (3, 4). The method takes advantage of the detection of the divergence in VP4 sequences both between and within serotypes, and thus is also of use for global epidemiologic studies of enteroviruses (1, 5, 7). We investigated the genetic diversity of CV-A16 strains associated with HFMD epidemics in the Fukushima Prefecture, Japan, from 1983 to 2003 and compared their genetic relation to those isolated in other areas of Japan and in China using the same method. CV-A16 strains isolated in Fukushima, from 1983 to 2003, made at least three distinct clusters on the phylogenetic tree. The three clusters were designated genogroups A, B, and C and were associated with the HFMD epidemics from 1984 to 1994 (including the 1985 and 1991 outbreaks), 1987 to 1998 (including the 1988 and 1998 outbreaks), and 1995 to 2003 (including the 1995 and 2002 outbreaks), respectively. The predominant genogroup was replaced with a new genogroup. CV-A16 strains within a genogroup gradually became genetically divergent in several epidemics. These results demonstrated that the introduction of a new genogroup in addition to the genetic divergence within a genogroup resulted in repeated HFMD outbreaks in Fukushima, Japan.

Each genogroup formed the same cluster with CV-A16 strains isolated during essentially the same time period in other areas of Japan and in China. The clustering seemed to be more closely related to the date of isolation than to the geographic location. Genetic diversities appeared randomly throughout

FIG. 2. Phylogram depicting the phylogenetic relationships on the basis of the VP4 sequence among 129 CV-A16 strains isolated in Fukushima from 1983 to 2003. Bootstrap analysis was performed by resampling the data sets 1,000 times. Bootstrap values greater than 70% were considered to be statistically significant for the grouping and were denoted in the figure. Isolated place, strain name, and isolated year were indicated. The GenBank accession number of one isolate to represent isolates with identical sequences is also indicated in parenthesis. CA-A16/G-10/51 is the prototype CV-A16 strain. The VP4 nucleotide sequence of prototype HEV71/BrCr/71 was used as an outgroup in the analysis.

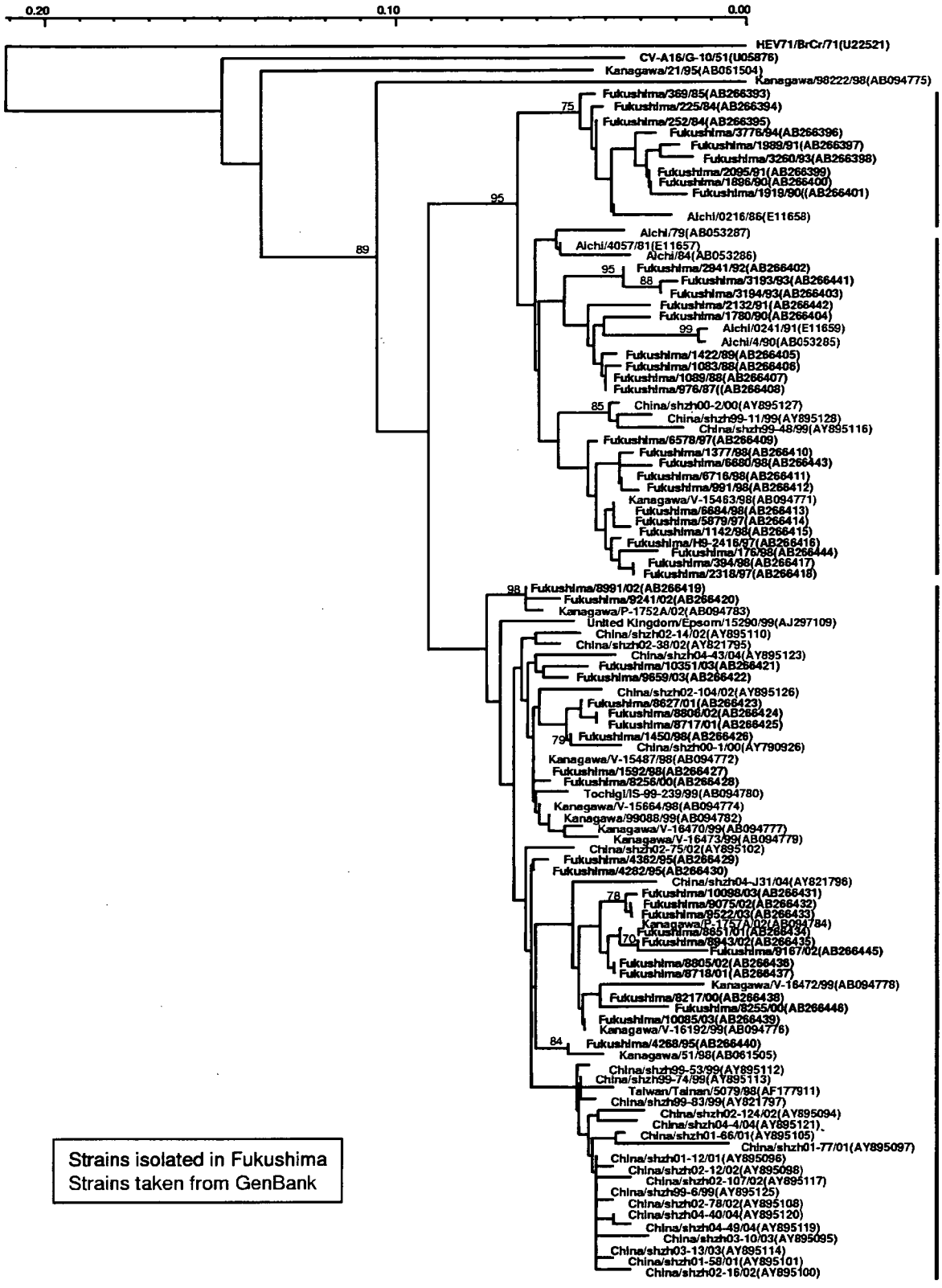

FIG. 3. Phylogram depicting the phylogenetic relationships on the basis of the VP4 sequence among representative 54 CV-A16 strains isolated in Fukushima and 50 CV-A16 strains isolated in Japan, China, and United Kingdom taken from international databases (GenBank). Bootstrap analysis was performed by resampling the data sets 1,000 times. Bootstrap values greater than 70% were considered to be statistically significant for the grouping and were denoted in the figure. Isolated place, strain name, and isolated year were indicated. GenBank accession numbers of CV-A16 strains isolated in Fukushima and the strains taken from international databases are indicated in parentheses. CA-A16/G-10/51 is the prototype CV-A16 strain. The VP4 nucleotide sequence of prototype HEV71/BrCr/71 was used as an outgroup in the analysis.

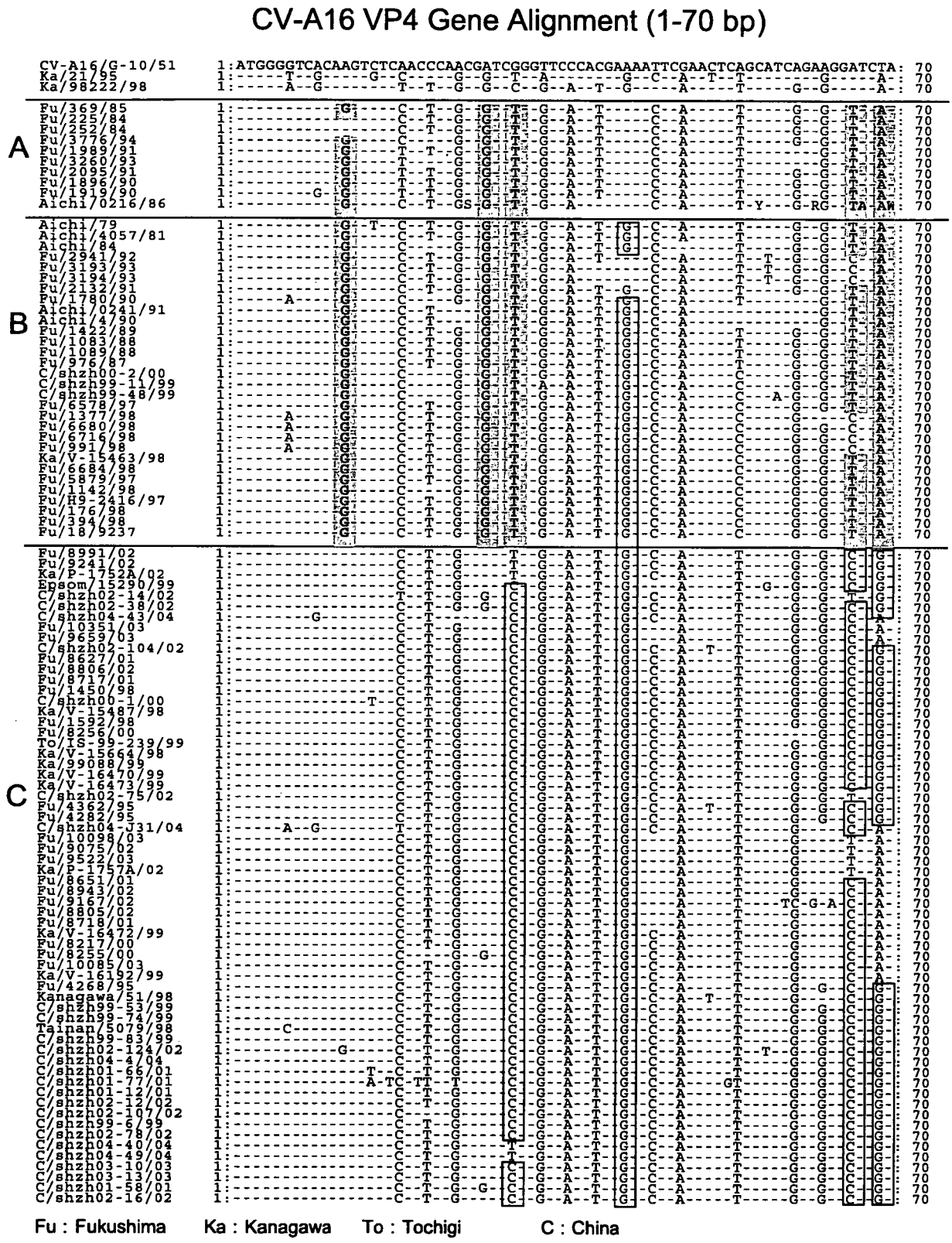

FIG. 4. Alignment of the entire VP4 sequences. Common genetic diversities were observed in each genogroup. Nucleotide differences from the prototype CV-A16/G-10/51 strain observed in genogroup A, genogroup A and B, or genogroup A and C are indicated by shading and those in genogroup B, genogroups B and C, or genogroup C are indicated in boxes.

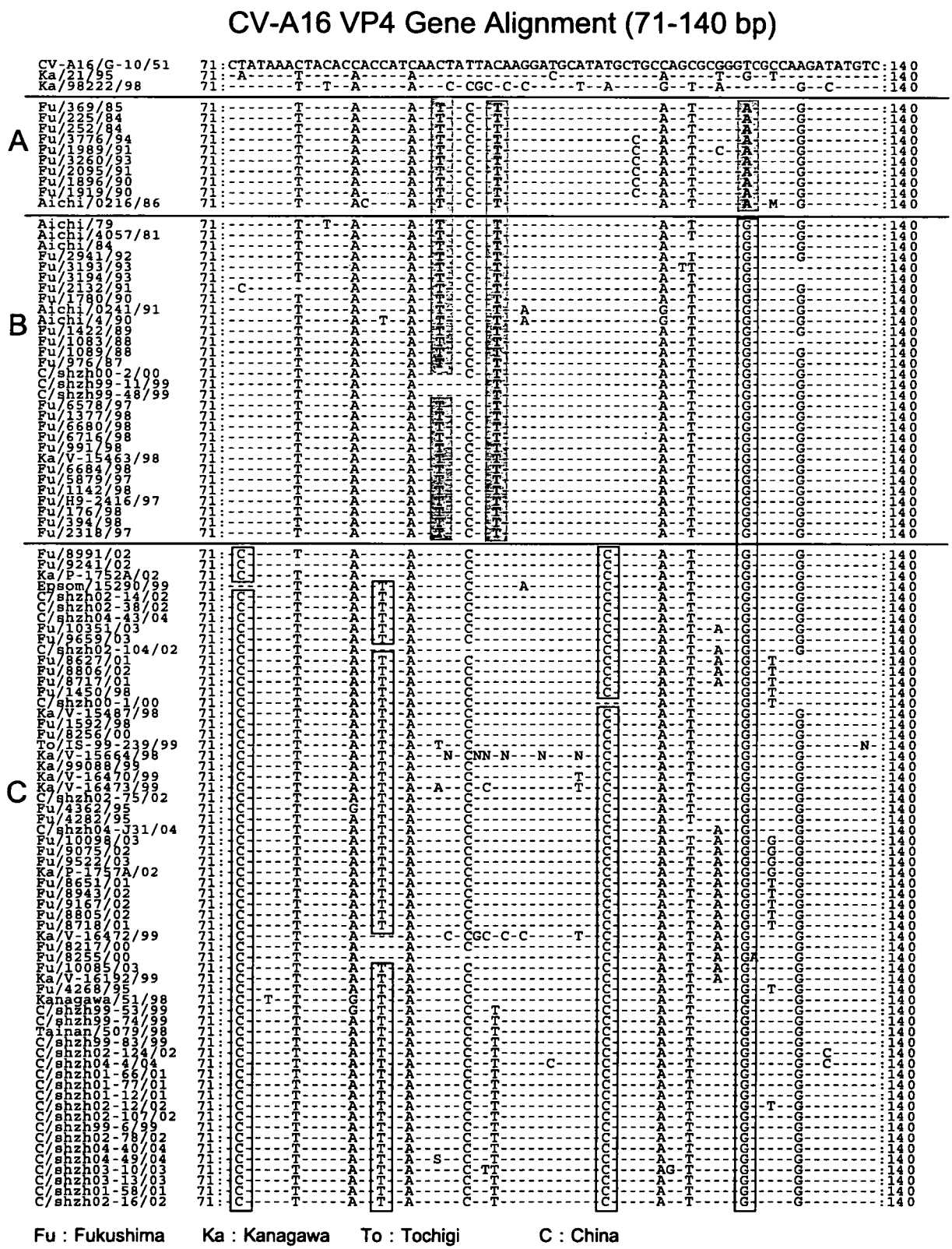

FIG. 4—*Continued.*

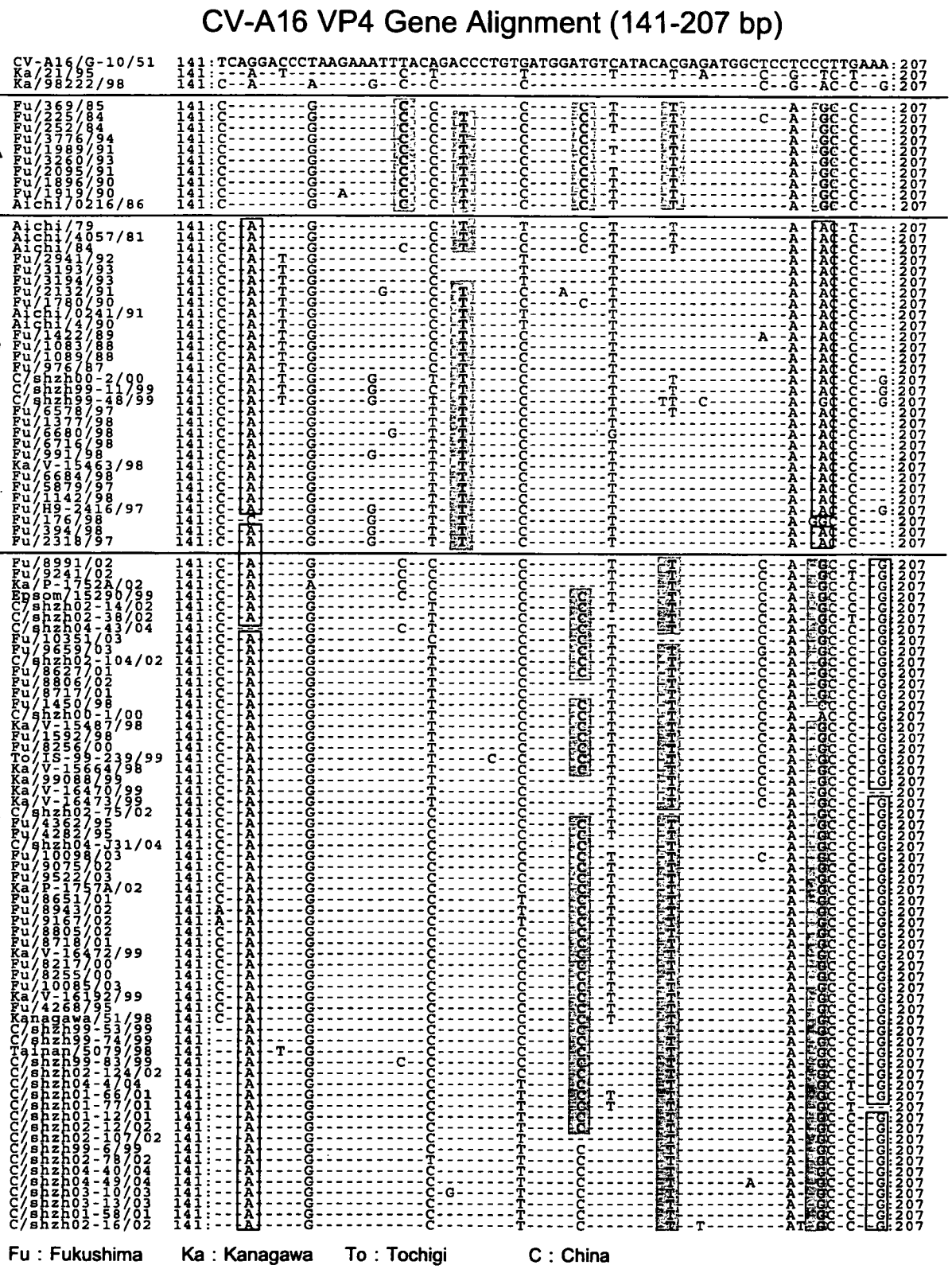

FIG. 4—*Continued.*

the VP4 gene and were common to each genogroup. These indicated that a new CV-A16 genogroup might derive from other regions of the world, be predominant for several years with genetic divergence, and then disappear.

The protein encoded by the VP1 gene is the most exposed and immunodominant of the capsid proteins. Serotypic identification and classification rely on antigenic methods, and VP1 gene sequence data are likely to give the most useful information in molecular epidemiologic studies (13). Shimizu et al. analyzed the phylogeny of HEV71 isolates, which is the other major etiologic agent of HFMD, based on the nucleotide sequence alignment of both the VP1 and VP4 regions (15). Phylogenetic trees based on VP4 sequences revealed that the HEV71 strains isolated from the Western Pacific Region formed two major genogroups, B and C, and were similar to those based on the VP1 sequences. Cardosa et al. reported that the VP1 and VP4 gene sequences both provide similar phylogenetic information, but the higher bootstrap values in the VP1 dendrograms provide greater confidence, particularly when elucidating new genotypes. Thus, the use of the shorter VP4 gene might be helpful for HEV71 surveillance, but the VP1 gene should be used for confirming data obtained with VP4-based analysis (1). Therefore, we confirmed the data obtained from the analysis based on VP4 genes of CV-A16 isolates by using VP1-based analysis. Phylogenetic analysis based on the VP1 gene demonstrated the existence of three genetically distinct groups, and the grouping was completely identical to the result obtained with VP4-based analysis. Bootstrap values for the grouping of A, B, and C based on the VP1 gene were higher than 80%, whereas those for the grouping of A and C based on the VP4 gene were higher than 70%. Although bootstrap values are slightly higher in the VP1 dendrograms than in the VP4 dendrograms, the VP4 gene as well as the VP1 gene seems to be appropriate for the epidemiologic study of CV-A16. In conclusion, phylogenetic analysis based on the VP1 gene confirmed that CV-A16 strains isolated in Fukushima formed three genogroups, and each genogroup formed the same cluster with CV-A16 strains isolated during essentially the same time period in China.

In summary, we describe the evident genetic diversity and changes in the VP4 protein region of CV-A16 strains that were isolated in a restricted region through more than 20 successive epidemics. Our results indicate that CV-A16 strains causing HFMD had genetically changed twice during the period and that these CV-A16 strains might have been transmitted overseas. We conclude that the repeated outbreaks of CV-A16-related HFMD might be caused, in part, by the worldwide transmission of the genetically changed CV-A16 strains, as well as a large cohort of nonimmune individuals. To test this hypothesis, a worldwide surveillance system for HFMD and genetic analysis of isolated CV-A16 strains is necessary.

ACKNOWLEDGMENT

We do not have a commercial or other association that might pose a conflict of interest (e.g., pharmaceutical stock ownership, consultancy, advisory board membership, relevant patents, or research funding).

REFERENCES

1. **Cardosa, M. J., D. Perera, B. A. Brown, D. Cheon, H. M. Chan, K. P. Chan, H. Cho, and P. McMinn.** 2003. Molecular epidemiology of human enterovirus 71 strains and recent outbreaks in the Asia-Pacific region: comparative analysis of the VP1 and VP4 genes. Emerg. Infect. Dis. **9**:461–468.
2. **Chang, L. Y., T. Y. Lin, Y. C. Huang, K. C. Tsao, S. R. Shih, M. L. Kuo, H. C. Ning, P. W. Chung, and C. M. Kang.** 1999. Comparison of enterovirus 71 and coxsackievirus A16 clinical illness during the Taiwan enterovirus epidemic, 1998. Pediatric. Infect. Dis. J. **18**:1092–1096.
3. **Hosoya, M., M. Sato, K. Honzumi, M. Katayose, Y. Kawasaki, H. Sakuma, K. Kato, Y. Shimada, H. Ishiko, and H. Suzuki.** 2001. Association of nonpolio enteroviral infection in the central nervous system of children with febrile seizures. Pediatrics **107**:E12.
4. **Hosoya, M., H. Ishiko, Y. Shimada, K. Honzumi, S. Suzuki, K. Kato, and H. Suzuki.** 2002. Diagnosis of group A coxsackieviral infection using polymerase chain reaction. Arch. Dis. Child. **87**:316–319.
5. **Hosoya, M., Y. Kawasaki, M. Sato, K. Honzumi, A. Kato, T. Hiroshima, H. Ishiko, and H. Suzuki.** 2006. Genetic diversity of enterovirus 71 associated with hand, foot, and mouth disease epidemics in Japan from1983 to 2003. Pediatr. Infect. Dis. J. **25**:691–694.
6. **Infectious Disease Surveillance Center.** 2004. Infectious agents surveillance report: enterovirus isolation from aseptic meningitis cases, 1982–2003, Tokyo, Japan. Infectious Disease Surveillance Center, Tokyo, Japan. (In Japanese.)
7. **Ishiko, H., Y. Shimada, M. Yonaha, O. Hashimoto, A. Hayashi, K. Sakae, and N. Takeda.** 2002. Molecular diagnosis of human enteroviruses by phylogeny-based classification by use of the VP4 sequence. J. Infect. Dis. **185**: 744–754.
8. **Kimura, M.** 1980. A simple method for estimating evolutionary rates of base substitutions through comparative studies of nucleotide sequences. J. Mol. Evol. **16**:111–120.
9. **Li, L., Y. He, H. Yang, J. Zhu, X. Xu, J. Dong, Y. Zhu, and Q. Jin.** 2005. Genetic characteristics of human enterovirus 71 and coxsackievirus A16 circulating from 1999 to 2004 in Shenzhen, People's Republic of China. J. Clin. Microbiol. **43**:3835–3839.
10. **McMinn, P., K. Lindsay, D. Perera, H. M. Chan, K. P. Chan, and M. J. Cardosa.** 2001. Phylogenetic analysis of enterovirus 71 strains isolated during linked epidemics in Malaysia, Singapore, and Western Australia. J. Virol. **75**:7732–7738.
11. **Nomoto, A., T. Omata, H. Toyoda, S. Kuge, H. Horie, Y. Kataoka, Y. Genba, Y. Nakano, and N. Imura.** 1982. Complete nucleotide sequence of the attenuated poliovirus Sabin 1 strain genome. Proc. Natl. Acad. Sci. USA **79**:5793–5797.
12. **Oberste, M. S., K. Maher, M. L. Kennett, J. J. Campbell, M. S. Carpenter, D. Schnurr, and M. A. Pallansch.** 1999. Molecular epidemiology and genetic diversity of echovirus type 30 (E30): genotypes correlate with temporal dynamics of E30 isolation. J. Clin. Microbiol. **37**:3928–3933.
13. **Oberste, M. S., K. Maher, D. A. Kilpatrick, and M. A. Pallansch.** 1999. Molecular evolution of the human enteroviruses: correlation of serotype with VP1 sequence and application to picornavirus classification. J. Virol. **73**:1941–1948.
14. **Saitou, N., and M. Nei.** 1987. The neighbor-joining method: a new method for reconstructing phylogenetic trees. Mol. Biol. Evol. **4**:406–425.
15. **Shimizu, H., A. Utama, N. Onnimala, C. Li, Z. Li-Bi, M. Yu-Jie, Y. Pongsuwanna, and T. Miyamura.** 2004. Molecular epidemiology of enterovirus 71 infection in the Western Pacific region. Pediatr. Int. **46**:231–235.

Nuclear factor-κB activation in peripheral blood mononuclear cells in children with sepsis

Noriko Hotta, MD; Takashi Ichiyama, MD; Masahiro Shiraishi, MD; Tsuyoshi Takekawa, MD; Tomoyo Matsubara, MD; Susumu Furukawa, MD

Objective: **To determine the activation of nuclear factor-κB in peripheral blood CD14+ monocyte/macrophages and CD3+, CD4+, and CD8+ T cells in children with sepsis.**

Design: **Observational study.**

Setting: **University hospital.**

Patients: **Twenty-six children with sepsis (nine females and 17 males, aged between 10 days and 15 yrs; median, 4.3 yrs) on admission to our hospital between August 1999 and November 2005.**

Interventions: **None.**

Measurements and Main Results: **The percentages of peripheral blood CD14+ monocyte/macrophages and CD3+, CD4+, and CD8+ T cells exhibiting nuclear factor-κB activity were determined by flow cytometry. In addition, relationships among the degree to which nuclear factor-κB was activated, serum levels of cytokines (interferon-γ, tumor necrosis factor-α, interleukin-2, interleukin-4, interleukin-6, and interleukin-10), and clinical variables were analyzed. The percentage of cells exhibiting nuclear factor-κB activity was increased among CD14+, CD3+, CD4+, and CD8+ cells in the sepsis group and was significantly higher among CD14+, CD3+, and CD4+ cells of the patients with severe sepsis (n = 9) than those of patients with nonsevere sepsis (n = 17). The percentage of cells exhibiting nuclear factor-κB activity was significantly higher among CD14+ cells than CD3+ cells in the patients with severe sepsis. In addition, this percentage was significantly higher among CD14+ cells than CD3+, CD4+, and CD8+ cells in septic patients who had positive blood cultures (n = 16). Serum interleukin-6 levels were correlated with the percentages of CD14+, CD3+, CD4+, and CD8+ cells exhibiting nuclear factor-κB activity, and serum IL-10 levels were correlated with the percentages of CD14+, CD3+, and CD4+ cells exhibiting nuclear factor-κB activity.**

Conclusions: **Nuclear factor-κB in peripheral blood mononuclear cells was activated in children with sepsis and was related the severity of sepsis. (Crit Care Med 2007; 35:2395–2401)**

KEY WORDS: **sepsis; children; NF-kappaB; interleukin-6; interleukin-10**

Despite many advances in therapeutic techniques, sepsis is still a severe and potentially lethal condition. Previous studies have demonstrated that the clinical condition of patients with sepsis is modified by the release of large amounts of proinflammatory cytokines, such as tumor necrosis factor (TNF)-α, interleukin (IL)-1, and IL-6, into the blood (1, 2).

Nuclear factor (NF)-κB is a ubiquitous transcription factor for genes that encode proinflammatory cytokines (3–7). The prototype of NF-κB is a heterodimer consisting of p50 and p65 bound by members of the IκB family, including IκBα, in the cytoplasm (8, 9). Phosphorylation of IκB by bacterial products, viruses, drugs, or cytokines rapidly leads to its degradation and the translocation of NF-κB to the nucleus (10, 11). Activation of NF-κB results in the binding of specific promoter elements and the expression of messenger RNAs for proinflammatory cytokine genes (10, 11).

To determine the role of NF-κB activation in children with sepsis, we measured the percentages of CD14+ monocyte/macrophages and CD3+, CD4+, and CD8+ T cells exhibiting NF-κB activity in the peripheral blood mononuclear cell (PBMC) population by flow cytometric analysis. In addition, relationships among the degree to which NF-κB was activated in PBMCs, serum proinflammatory cytokine concentrations, severity of sepsis, and clinical variables were analyzed in children with sepsis.

MATERIALS AND METHODS

Sepsis. Informed consent was obtained from the parents of the patients enrolled in this study. The protocol was approved by the Institutional Review Board of Yamaguchi University Hospital. Peripheral blood samples were obtained from 26 children with sepsis (nine females and 17 males, aged between 10 days and 15 yrs; median, 4.3 yrs) on admission to our hospital between August 1999 and November 2005 (Table 1). Septic children who did not receive any antibiotics before blood sampling and provided blood samples within 5 days from the onset of the illness were enrolled in our study. Sepsis for a pediatric population was defined as systemic inflammatory response syndrome in the presence of or as a result of suspected or proven infection (12). Systemic inflammatory response syndrome was defined as the presence of at least two of the following four criteria, one of which must be an abnormal temperature or leukocyte count: 1) hyperthermia or hypothermia; 2) tachycardia or bradycardia; 3) tachypnea; 4) an elevated or depressed leukocyte count (12). Severe sepsis was defined as sepsis plus one of the following: cardiovascular organ dysfunc-

From the Department of Pediatrics, Yamaguchi University Graduate School of Medicine, Yamaguchi, Japan.

The authors certify that there is no financial assistance related to this study. The authors have not disclosed any potential conflicts of interest.

For information regarding this article, E-mail: ichiyama@yamaguchi-u.ac.jp

DOI: 10.1097/01.CCM.0000284502.38701.E6

Table 1. Clinical characteristics of 26 patients with sepsis and controls

	Severe Sepsis (n = 9)		Nonsevere Sepsis (n = 17)		Control (n = 18)
Age, median, range	1.9 yrs, 27 days–15 yrs		5.5 yrs, 10 days–15 yrs		3.2 yrs, 26 days–13 yrs
Sex, female:male	3:6		6:11		7:11
Type of infection	Meningitis	3	Pneumonia	8	
	Catheter-related infection	2	Bronchitis	3	
	Pneumonia	2	Acute otitis media	1	
	Enterocolitis	1	Arthritis of the hip	1	
	UTI	1	Enterocolitis	1	
			Meningitis	1	
			Meningoencephalitis	1	
			UTI	1	
Primary causative bacteria	*Haemophilus influenzae*	3	*Haemophilus influenzae*	6	
	MRSA	2	MSSA	2	
	Enterobacter aerogenes	1	*Escherichia coli*	1	
	Escherichia coli	1	MRSA	1	
	MRSE	1	*Pseudomonas aeruginosa*	1	
	Pseudomonas aeruginosa	1	*Streptococcus pyogenes*	1	
			Unknown	5	
Blood culture	Positive	8	Positive	8	
	Negative	1	Negative	9	
Sampling days, median, range	3, 1–5		3, 1–5		
Comorbid conditions	Cerebral palsy	2	Cerebral palsy	4	
	Acute encephalopathy	1			
	Lowe syndrome	1			

UTI, urinary tract infection; MRSA, methicillin-resistant *Staphylococcus aureus;* MSSA, methicillin-sensitive *Staphylococcus aureus*; MRSE, methicillin-resistant *Staphylococcus epidermidis.*

The day of fever onset was considered to be the first day of illness.

tion, acute respiratory distress syndrome, or two or more other organ dysfunctions, including neurologic, hematologic, renal, and hepatic dysfunction (12). The day of fever onset was considered as the first day of illness. Twenty patients had fever before admission, and six patients had fever while their original diseases were treated in the hospital. Blood samples were obtained from patients with sepsis on days 1 through 5 (mean, 2.9 days) of illness and as soon as they were diagnosed as having sepsis.

Controls. The control subjects were 18 healthy children (11 males and seven females, aged between 26 days and 13 yrs; median, 3.2 yrs). They included children who were undergoing surgery (for inguinal hernia, strabismus) and those who were brought for blood type determination. There were no significant differences of age or gender between septic children and healthy controls by the Mann-Whitney U test.

Flow Cytometric Analysis. The flow cytometric analysis was performed according to a previously published procedure (13–15). Peripheral blood cells were labeled with a phycoerythrin-conjugated anti-CD14 monoclonal antibody, a peridinin chlorophyll protein-conjugated anti-CD3 monoclonal antibody, a phycoerythrin-conjugated anti-CD4 monoclonal antibody, or a peridinin chlorophyll protein-conjugated anti-CD8 monoclonal antibody and then permeabilized with 4%

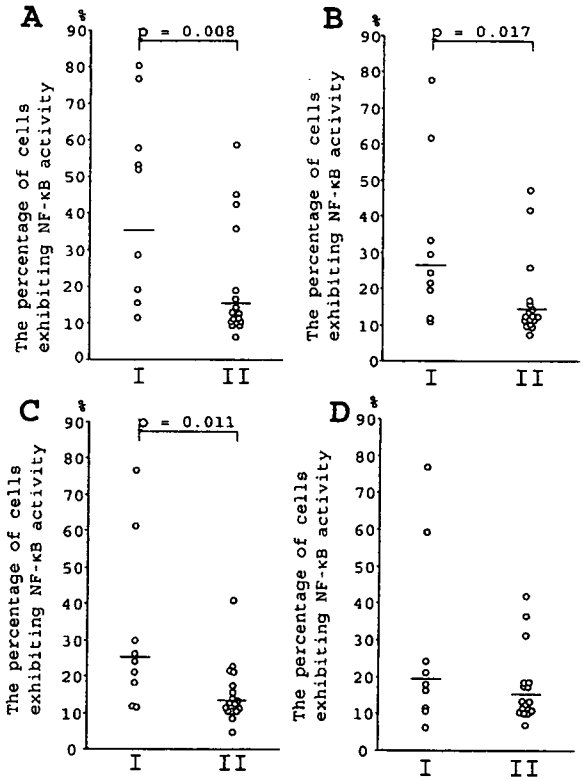

Figure 1. The percentage of CD14+ (*A*), CD3+ (*B*), CD4+ (*C*), and CD8+ (*D*) cells exhibiting nuclear factor (*NF*)-κB activity. *I*, patients with severe sepsis (n = 9); *II*, patients with nonsevere sepsis (n = 17). Horizontal lines are geometric mean values.

paraformaldehyde in phosphate-buffered saline, pH 7.2, containing 0.1% saponin and 10 mM HEPES. The cells were labeled with mouse anti-NF-κB (nuclear-localized signal) antibody (immunoglobulin G3; CHEMICON, Temecula, CA). The mouse anti-NF-κB (nuclear-localized signal) antibody recognizes an epitope overlapping the nuclear location signal of NF-κB-p65 and therefore selectively recognizes the activated form of NF-κB. The cells were then labeled with a fluorescein isothiocyanate-conjugated rat anti-mouse immunoglobulin G3 monoclonal antibody (BD PharMingen, San Diego, CA). After being washed, the cells were fixed with 1% paraformaldehyde in phosphate-buffered saline and stored at 4°C until the flow cytometric analysis. Immunofluorescence staining was analyzed with a FACScan flow cytometer equipped with CellQuest software. We analyzed 5,000 cells by flow cytometry for each patient.

Determination of Cytokine Concentrations. The concentrations of interferon (IFN)-γ, TNF-α, IL-2, IL-4, IL-6, and IL-10 in serum were measured with a cytometric bead array kit (BD PharMingen) according to the manufacturer's manual, as described previously (16–18), with modifications of the data analysis using GraphPad Prism software (GraphPad Prism Software, San Diego, CA). Briefly, a cytometric bead array comprises a series of beads exhibiting discrete fluorescence intensities at 670 nm. Each series of beads is coated with a monoclonal antibody against a single cytokine, and a mixture of six series of beads can detect six cytokines in one sample. A secondary phycoerythrin-conjugated monoclonal antibody stains the beads proportionally to the amount of bound cytokine. After fluorescence intensity calibration and electronic color compensation procedures, standard and test samples were analyzed with a FACScan flow cytometer equipped with CellQuest software (BD PharMingen), and the data were transferred to GraphPad Prism. Starting with standard dilutions, the software performed log transformations of the data and then fitted a curve to ten discrete points using a four-variable logistic model. The calibration curve created for each cytokine was used to determine the cytokine concentrations in the samples. The lower detection limits for IFN-γ, TNF-α, IL-2, IL-4, IL-6, and IL-10 were 7.1 pg/mL, 2.8 pg/mL, 2.6 pg/mL, 2.6 pg/mL, 2.5 pg/mL, and 2.8 pg/mL, respectively.

Clinical Data. The relationships among the percentages of cells exhibiting NF-κB activity and clinical data, including the species of causative bacteria, white blood cell counts, platelet counts, serum C-reactive protein, body temperature, heart rate, respiratory rate, blood pressure at the time of specimen collection, and aspartate aminotransferase, alanine aminotransferase, and lactate dehydrogenase levels, were investigated. Disseminated intravascular coagulation was diagnosed as in a previous paper (19). Moreover, the Pediatric Risk of Mortality score (20) was calculated.

Statistical Analysis. All data were log transformed to get an approximately normal distribution. The differences in the results between groups were analyzed with a *t*-test, and those with a p value $<.05$ were considered significant. Correlations were analyzed using Pearson's coefficient correlation. All values are geometric means. Analyses and calculations were performed using SPSS-12.0 (SPSS, Chicago, IL).

RESULTS

Patients With Sepsis. Clinical data of patients with sepsis are shown in Table 1. Type of infection included pneumonia (n = 10), bacterial meningitis (n = 4), acute bronchitis (n = 3), acute enterocolitis (n = 2), urinary tract infection (n = 2), catheter-related infection (n = 2), encephalomeningitis (n = 1), acute otitis media (n = 1), and arthritis of the hip (n = 1). Nine of the 26 septic children had severe sepsis. Blood cultures yielded *Haemophilus influenzae* (n = 6), methicillin-resistant *Staphylococcus aureus* (n = 3), *Escherichia coli* (n = 2), *Pseudomonas aeruginosa* (n = 2), *Enterobacter aerogenes* (n = 1), methicillin-sensitive *S. aureus* (n = 1), and *Streptococcus pyogenes* (n = 1). Blood cultures from ten septic patients were negative. The comorbid conditions of the patients included cerebral palsy (n = 6), acute encephalopathy (n = 1), and Lowe syn-

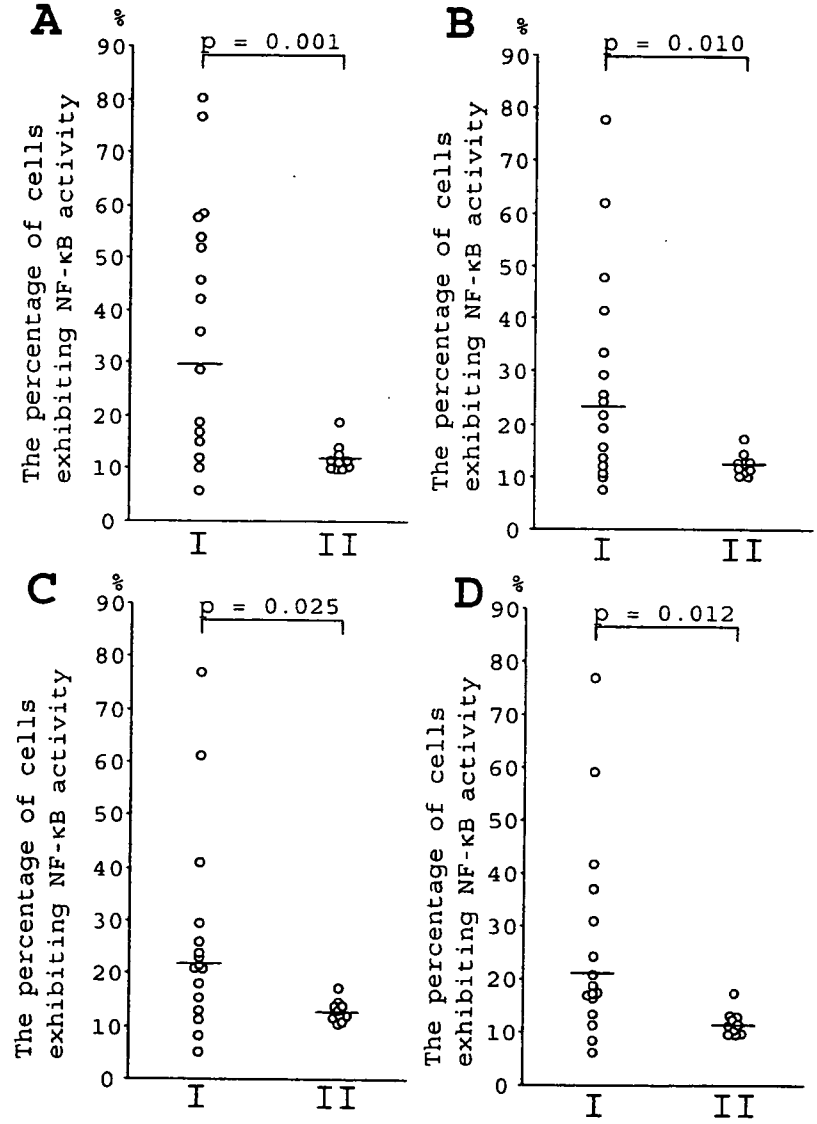

Figure 2. Relationship between blood culture and the percentage of CD14+ (*A*), CD3+ (*B*), CD4+ (*C*), and CD8+ (*D*) cells exhibiting nuclear factor (*NF*)-κB activity. *I*, patients with positive blood cultures (n = 16); *II*, patients with negative blood cultures (n = 10). Horizontal lines are geometric mean values.

drome (n = 1). The other 18 patients were healthy before having infections complicated with sepsis. Three cases of severe sepsis and one of nonsevere sepsis were complicated with disseminated intravascular coagulation. The patients were treated with multiple antibiotics effective against these bacteria. One male patient aged 27 days with severe sepsis died 3 days after specimen collection, and the other 25 patients survived without sequelae.

Percentage of Cells Exhibiting NF-κB Activity. The percentages of CD14+, CD3+, CD4+, and CD8+ cells exhibiting NF-κB activity among the controls were 2.4%, 2.6%, 2.3%, and 2.2%, respectively (Fig. 1). Those of CD14+, CD3+, CD4+, and CD8+ cells from the patients in the sepsis group were significantly higher: 21.0%, 18.0%, 17.0%, and 16.8%, respectively (all $p < .001$). The percentages of CD14+, CD3+, and CD4+ cells exhibiting NF-κB activity were significantly higher in the patients with severe sepsis than those with nonsevere sepsis ($p = .008$, $p = .017$, and $p = .011$, respectively), but not so for the percentage of CD8+ cells (Fig. 1). A logistic regression analysis demonstrated that the percentages of CD14+, CD3+, and CD4+ cells, but not CD8+ cells, exhibiting NF-κB activity were significantly higher in the patients with severe sepsis than those with nonsevere sepsis ($p = .023$, $p = 0034$, and $p = .034$, respectively) after adjustment for age, gender, and sampling days. In the patients with severe sepsis, the percentage was significantly higher among CD14+ cells than CD3+ cells ($p = .037$).

The percentages of CD14+, CD3+, CD4+, and CD8+ cells exhibiting NF-κB activity were significantly higher in septic patients who had positive blood cultures than those who had negative blood cultures ($p = .001$, $p = .010$, $p = .025$, and $p = .012$, respectively) (Fig. 2). In the septic patients who had positive blood cultures, the percentage of cells exhibiting NF-κB activity was significantly higher among CD14+ cells than CD3+ ($p = .006$), CD4+ ($p = .011$), or CD8+ ($p = .028$) cells. There was no significant difference in the percentages of cells exhibiting NF-κB activity between the septic patients who tested positive in the blood culture for *H. influenzae* (n = 6) and the others (n = 10).

The percentages of CD14+, CD3+, CD4+, and CD8+ cells exhibiting NF-κB activity were significantly higher in the septic patients with disseminated intravascular coagulation (n = 4) than those without disseminated intravascular coagulation ($p = .007$, $p < .001$, $p < .001$, and $p = .011$, respectively). There was no significant correlation between the percentages of cells exhibiting NF-κB activity and differential white blood cell counts, serum C-reactive protein, body temperature, heart rate, respiratory rate, blood pressure, or aspartate aminotransferase, alanine aminotransferase, or lactate dehydrogenase levels at the time of specimen collection. There were no significant correlations between the percentages of cells exhibiting NF-κB activ-

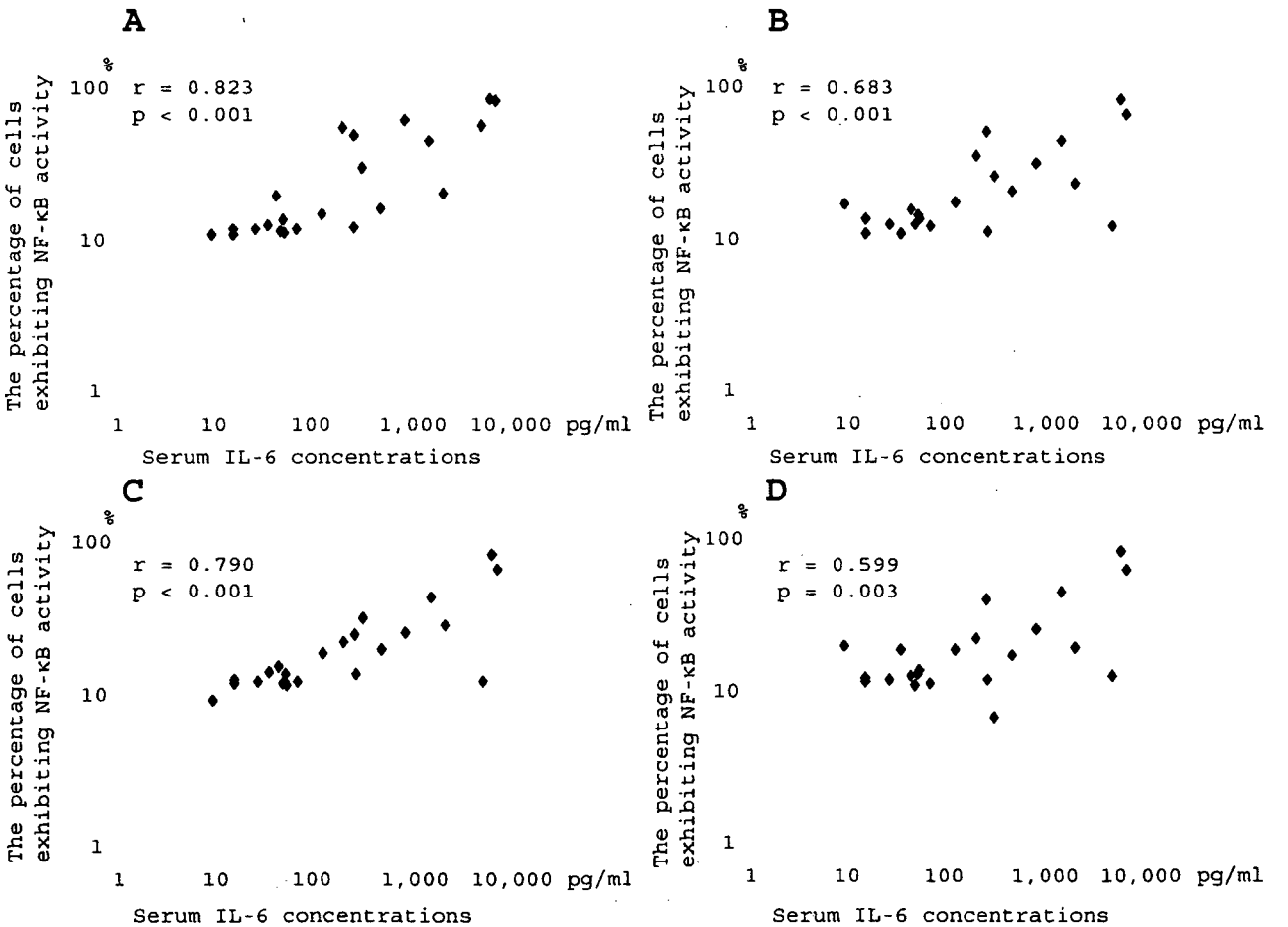

Figure 3. Relationship between serum interleukin (*IL*)-6 levels and the percentages of CD14+ (*A*), CD3+ (*B*), CD4+ (*C*), and CD8+ (*D*) cells exhibiting nuclear factor (*NF*)-κB activity. *r*, Pearson's coefficient.

ity and Pediatric Risk of Mortality scores in the patients. The Pediatric Risk of Mortality score of patients with severe sepsis was significantly higher than that of patients with nonsevere sepsis ($p = .007$; median, range: 6, 0–29 vs. 0, 0–8).

The concentrations of IFN-γ, TNF-α, IL-2, IL-4, IL-6, and IL-10 in the serum of the control subjects were <42.9 pg/mL, <11.1 pg/mL, <4.5 pg/mL, <15.0 pg/mL, <19.9 pg/mL, and <14.2 pg/mL, respectively. Serum cytokine levels were determined in 22 of the 26 patients. Serum IL-6 levels were elevated in 21 of the 22 patients (15.8–9701 pg/mL) and were correlated with the percentage of cells exhibiting NF-κB activity among CD14+ ($r = 0.823$, $p < .001$), CD3+ ($r = 0.683$, $p < .001$), CD4+ ($r = 0.790$, $p < .001$), and CD8+ ($r = 0.599$, $p = .003$) cells (Fig. 3). Serum IL-10 levels were elevated in 12 of the 22 patients (15.3–302.8 pg/mL) and were correlated with the percentage of cells exhibiting NF-κB activity among CD14+ ($r = 0.702$, $p < .001$), CD3+ ($r = 0.525$, $p = .012$), and CD4+ cells ($r = 0.628$, $p = .002$), but not CD8+ cells (Fig. 4). Serum IFN-γ, TNF-α, IL-2, and IL-4 levels were elevated in two (76.6 and 509.4 pg/mL), three (93.4 to 306.8 pg/mL), one (4.7 pg/mL), and five (21.1 to 50.9 pg/mL) of the 22 patients, respectively. There was no correlation between the percentage of cells exhibiting NF-κB activity in the PBMC population and serum IFN-γ, TNF-α, IL-2, or IL-4 levels.

DISCUSSION

Previous studies have revealed that NF-κB in PBMCs is activated in adult patients with sepsis (21–25). Levels of NF-κB activity were higher in the PBMCs of nonsurvivors than those of survivors (21–23). An analysis of each cell type in the PBMC population has not been performed. Moreover, no pediatric sepsis studies related specifically to the activation of NF-κB have been reported.

We investigated the correlation between the percentages of cells exhibiting NF-κB activity in the PBMC population and the severity of sepsis in children, although this was not an age- or gender-matched control study. The percentages of CD14+, CD3+, and CD4+ cells exhibiting NF-κB activity were significantly higher in patients with severe sepsis than those with nonsevere sepsis. Several variables are used to assess the severity of sepsis (12, 26, 27). The percentages of cells exhibiting NF-κB activity in the PBMC population were related to the severity of sepsis defined by the International Pediatric Sepsis Consensus Conference, although children with more severe sepsis having high Pediatric Risk of Mortality scores might be investigated (12, 20). Therefore, it is likely that the percentage among PBMCs is a marker of the severity of sepsis; in fact, one patient who died had markedly elevated percentages of cells exhibiting NF-κB activity among PBMCs (CD14+, 77%; CD3+, 62%; CD4+, 61%; CD8+, 59%). However, the sampling period in the present study was 1–5 days after the onset of fever. Duration

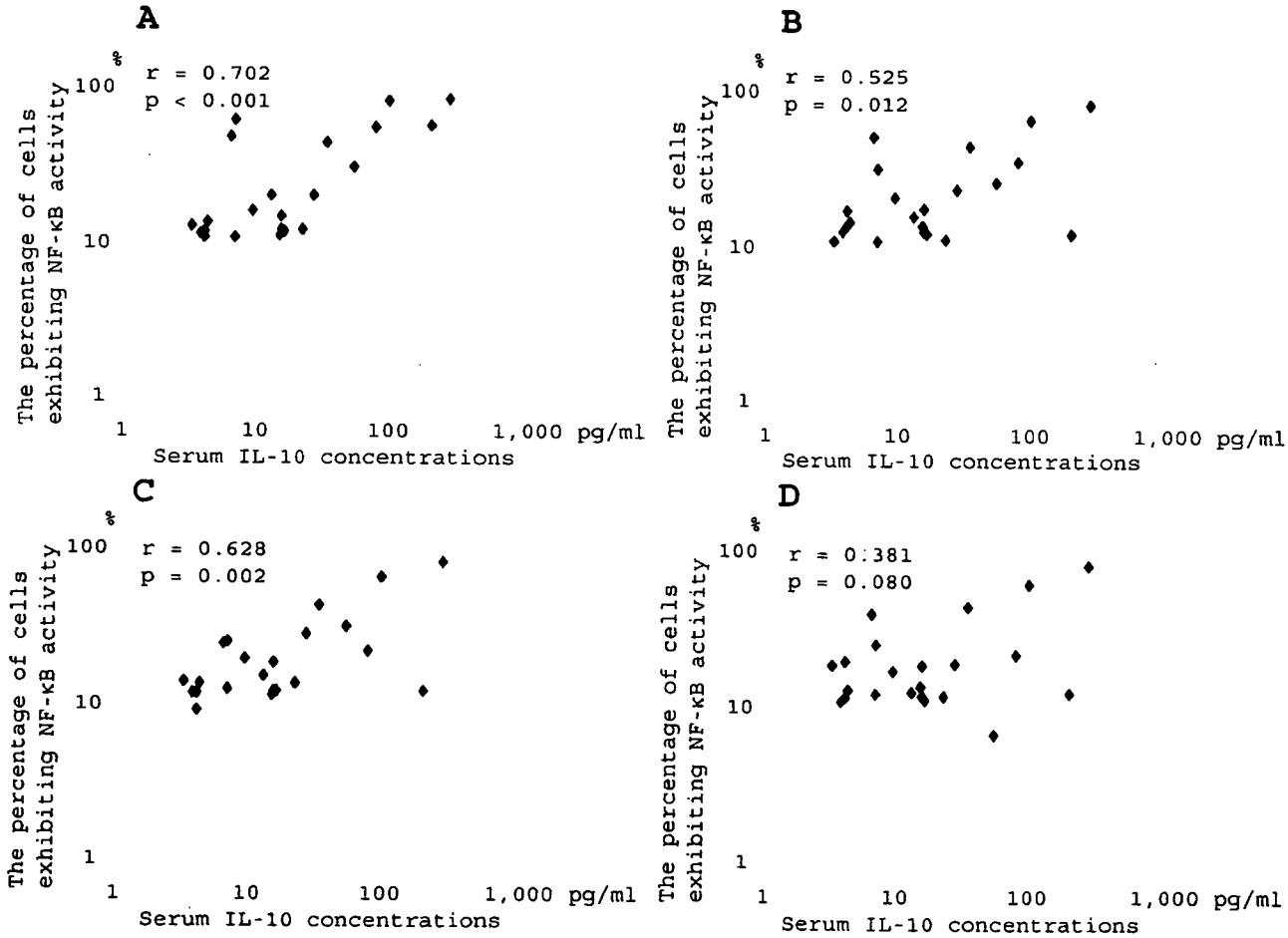

Figure 4. Relationship between serum interleukin (*IL*)-10 levels and the percentages of CD14+ (*A*), CD3+ (*B*), CD4+ (*C*), and CD8+ (*D*) cells exhibiting nuclear factor (*NF*)-κB activity. *r*, Pearson's coefficient.

of fever may affect the percentages of cells exhibiting NF-κB activity in the PBMC population.

Sixteen of 26 septic children in the present study had positive blood cultures. The percentages of cells exhibiting NF-κB activity among CD14+, CD3+, CD4+, and CD8+ cells were significantly higher in the septic patients who had positive blood cultures than those who had negative blood cultures. There was no significant difference in the percentages of cells exhibiting NF-κB activity with the type of causative bacteria in this study. However, a further large-scale study is necessary to clarify the relationship between NF-κB's activation and types of causative bacteria.

We investigated for the first time the activation of NF-κB in CD14+, CD3+, CD4+, and CD8+ cells of children with sepsis individually. The percentage of cells exhibiting NF-κB activity was increased among all four types of cells and was significantly higher among CD14+ monocyte/macrophages than CD3+ T cells in children with severe sepsis. In addition, the percentage was significantly higher among CD14+ cells than CD3+, CD4+, and CD8+ cells in septic children who had positive blood cultures. Unlike CD3+, CD4+, and CD8+ cells, CD14+ cells show a direct defensive response to bacterial infection without mediation by the major histocompatibility complex (28). As a result, CD14+ cells recognize antigens earlier than other cells. It is likely that the activation of CD14+ cells results in an immediately higher percentage of cells exhibiting NF-κB activity.

IL-6 is a cytokine that plays important roles in inflammatory responses and is recognized as a primary mediator in the pathogenesis of inflammation (29). Several previous reports investigated plasma and serum IL-6 levels of septic patients (30–35). We revealed that serum IL-6 and IL-10 levels were correlated with the percentage of cells exhibiting NF-κB activity in the PBMC population, with CD14+ monocytes/macrophages having the highest correlation. IL-10, as an anti-inflammatory cytokine, decreases the production of IL-1, IL-6, and TNF-α induced by endotoxins or bacteria (36, 37). Moreover, IL-10 can modulate NF-κB activation (38). Therefore, we suggest that IL-10 is produced in response to the overexpression of IL-6 and activation of NF-κB to modulate the production of cytokines during sepsis, and the level of IL-10 may reflect the degree of production of proinflammatory cytokines and NF-κB activation. However, it is difficult to clarify a causal relationship between NF-κB activation and serum IL-6 and IL-10 levels given the limitations of the study design.

CONCLUSIONS

NF-κB in CD14+ monocytes/macrophages and in CD3+, CD4+, and CD8+ T cells is activated in septic children, and this is related to the severity of the sepsis. The present findings suggest that PBMCs, especially CD14+ monocytes/macrophages, play important roles in the pathogenesis of pediatric sepsis.

ACKNOWLEDGMENT

We thank Prof. M. Okuda (Department of Pubic Health, Yamaguchi University Graduate School of Medicine) for his assistance with the statistical analysis.

REFERENCES

1. Casey LC, Balk RA, Bone RC: Plasma cytokine and endotoxin levels correlate with survival in patients with the sepsis syndrome. *Ann Intern Med* 1993; 119:771–778
2. Damas P, Canivet JL, de Groote D, et al: Sepsis and serum cytokine concentrations. *Crit Care Med* 1997; 25:405–412
3. Collart MA, Baeuerle P, Vassali P: Regulation of tumor necrosis factor alpha transcription in macrophages: Involvement of four κB-like motifs and of constitutive and inducible forms of NF-κB. *Mol Cell Biol* 1990; 10: 1498–1506
4. Libermann TA, Baltimore D: Activation of interleukin-6 gene expression through the NF-κB transcription factor. *Mol Cell Biol* 1990; 10:2327–2334
5. Hiscott J, Marois J, Garoufalis J, et al: Characterization of a functional NF-κB site in the human interleukin 1β promotor: Evidence for a positive autoregulatory loop. *Mol Cell Biol* 1993; 13:6231–6240
6. Matsusaka T, Fujikawa K, Nishio Y, et al: Transcription factors NF-IL6 and NF-κB synergistically activate transcription of the inflammatory cytokines, interleukin 6 and interleukin 8. *Proc Natl Acad Sci U S A* 1993; 90:10193–10197
7. Kunsch C, Lang RK, Rosen CA, Shannon MF: Synergistic transcriptional activation of the IL-8 gene by NF-κB p65 (RelA) and NF-IL-6. *J Immunol* 1994; 153:153–164
8. Baeuerle PA, Henkel T: Function and activation of NF-κB in the immune system. *Annu Rev Immunol* 1994; 12:141–179
9. Baldwin AS Jr: The NF-κB and IκB proteins: New discoveries and insights. *Annu Rev Immunol* 1996;14: 649–683
10. Brown K, Gerstberger S, Carlson L, et al: Control of IκB-α proteolysis by site-specific, signal-induced phosphorylation. *Science* 1995; 267:1485–1488
11. Kumar A, Haque J, Lacoste J, et al: Double-stranded RNA-dependent protein kinase activates transcription factor NF-κB by phosphorylating IκB. *Proc Natl Acad Sci U S A* 1994; 91:6288–6292
12. Goldstein B, Giroir B, Randolph A: International Pediatric Sepsis Consensus Conference. Definitions for sepsis and organ dysfunction in pediatrics. *Pediatr Crit Care Med* 2005;6:2–8
13. Pyatt DW, Stillman WS, Yang Y, et al: An essential role for NF-κB in human CD34+ bone marrow cell survival. *Blood* 1999; 93: 3302–3308
14. Ichiyama T, Nishikawa M, Yoshitomi T, et al: Clarithromycin inhibits NF-κB activation in human peripheral blood mononuclear cells and pulmonary epithelial cells. *Antimicrob Agents Chemother* 2001; 45:44–47
15. Ichiyama T, Yoshitomi T, Nishikawa M, et al: NF-κB activation in peripheral blood monocytes/macrophages and T cells during acute Kawasaki disease. *Clin Immunol* 2001; 99: 373–377
16. Chen R, Lowe L, Wilson JD, et al: Simultaneous quantification of six human cytokines in a single sample using microparticle-based flow cytometric technology. *Clin Chem* 1999; 45:1693–1694
17. Cook EB, Stahl JL, Lowe L, et al: Simultaneous measurement of six cytokines in a single sample of human tears using microparticle-based flow cytometry: Allergics vs. non-allergics. *J Immunol Methods* 2001; 254:109–118
18. Metelitsa LS, Naidenk OV, Kant A, et al: Human NKT cells mediate antitumor cytotoxicity directly by recognizing target cell CD1d with bound ligand or indirectly by producing IL-2 to activate NK cells. *J Immunol* 2001; 167:3114–3122
19. Angstwurm MW, Dempfle CE, Spannagl M: New disseminated intravascular coagulation score: A useful tool to predict mortality in comparison with Acute Physiology and Chronic Health Evaluation II and Logistic Organ Dysfunction scores. *Crit Care Med* 2006; 34:314–320
20. Leteurtre S, Leclerc F, Martinot A, et al: Can generic scores (Pediatric Risk of Mortality and Pediatric Index of Mortality) replace specific scores in predicting the outcome of presumed meningococcal septic shock in children. *Crit Care Med* 2001; 29:1239–1245
21. Böhrer H, Qui F, Zimmermann T, et al: Role of NFκB in the mortality of sepsis. *J Clin Invest* 1997; 100:972–985
22. Arnalich F, Garcia-Palomero E, Lopez J, et al: Predictive value of nuclear factor κB activity and plasma cytokine levels in patients with sepsis. *Infect Immun* 2000; 68:1942–1945
23. Paterson RL, Galley HF, Dhillon JK, et al:

Increased nuclear factor κB activation in critically ill patients who die. *Crit Care Med* 2000; 28:1047–1051
24. van Leeuwen HJ, van der Bruggen T, van Asbeck BS, et al: Effect of corticosteroids on nuclear factor-κB activation and hemodynamics in late septic shock. *Crit Care Med* 2001; 29:1074–1077
25. Liu SF, Malik AB: NF-κB activation as a pathological mechanism of septic shock and inflammation. *Am J Physiol Lung Cell Mol Physiol* 2006; 290:L622–L645
26. Marshall JC, Cook DJ, Christou NV, et al: Multiple organ dysfunction score: A reliable descriptor of a complex clinical outcome. *Crit Care Med* 1995; 23:1638–1652
27. Shapiro NI, Wolfe RE, Moore RB, et al: Mortality in Emergency Department Sepsis (MEDS) score: A prospectively derived and validated clinical prediction rule. *Crit Care Med* 2003; 31:670–675
28. Kaplan SL: Bacteremia and septic shock. *In:* Textbook of Pediatric Infectious Diseases. Fifth Edition. Feigin RD, Cherry JD, Demmler GJ, et al (Eds). Philadelphia, Saunders, 2004, pp 810–825
29. Heinrich PC, Castell JV, Andus T: Interleukin-6 and the acute phase response. *Biochem J* 1990; 265:621–636
30. Krafte-Jacobs B, Bock GH: Circulating erythropoietin and interleukin-6 concentrations increase in critically ill children with sepsis and septic shock. *Crit Care Med* 1996; 24: 1455–1459
31. Pavcnik-Arnol M, Hojker S, Derganc M: Lipopolysaccharide-binding protein in critically ill neonates and children with suspected infection: Comparison with procalcitonin, interleukin-6, and C-reactive protein. *Intensive Care Med* 2004; 30:1454–1460
32. Pathan N, Williams EJ, Oragui EE, et al: Changes in the interleukin-6/soluble interleukin-6 receptor axis in meningococcal septic shock. *Crit Care Med* 2005; 33: 1839–1844
33. Oda S, Hirasawa H, Shiga H, et al: Sequential measurement of IL-6 blood levels in patients with systemic inflammatory response syndrome (SIRS)/sepsis. *Cytokine* 2005; 29: 169–175
34. Fida NM, Al-Mughales J, Farouq M: Interleukin-1α, interleukin-6 and tumor necrosis factor-α levels in children with sepsis and meningitis. *Pediatr Int* 2006; 48:118–124
35. Khassawneh M, Hayajneh WA, Kofahi H, et al: Diagnostic markers for neonatal sepsis: Comparing C-reactive protein, interleukin-6 and immunoglobulin M. *Scand J Immunol* 2007; 65:171–175
36. Howard M, Muchamuel T, Andrade S, et al: Interleukin 10 protects mice from lethal endotoxemia. *J Exp Med* 1993; 177:1205–1208
37. Paris MM, Hickey SM, Trujillo M, et al: The effect of interleukin-10 on meningeal inflammation in experimental bacterial meningitis. *J Infect Dis* 1997; 176:1239–1246
38. Wang P, Wu P, Siegel MI, et al: Interleukin (IL)-10 inhibits nuclear factor κB (NF κB) activation in human monocytes: IL-10 and IL-4 suppress cytokine synthesis by different mechanisms. *J Biol Chem* 1995; 270: 9558–9563

Clinical and Experimental Allergy, 37, 608–614

ORIGINAL PAPER

Cysteinyl leukotrienes enhance tumour necrosis factor-α-induced matrix metalloproteinase-9 in human monocytes/macrophages

T. Ichiyama, M. Kajimoto, M. Hasegawa, K. Hashimoto, T. Matsubara and S. Furukawa
Department of Pediatrics, Yamaguchi University School of Medicine, Yamaguchi, Japan

Summary

Background Matrix metalloproteinase-9 (MMP-9) is an important enzyme responsible for airway remodelling. Monocytes/macrophages have a cysteinyl leukotriene 1 (cysLT1) receptor, but its function is poorly understood.

Objective To elucidate the function of the cysLT1 receptor of human monocytes/macrophages in MMP-9 production.

Methods We examined the effect of cysLTs (LTC4, -D4 and -E4) on TNF-α-induced MMP-9 production in THP-1 cells, a human monocytic leukaemia cell line and peripheral blood $CD14^+$ monocytes/macrophages. In addition, we examined the effect of pranlukast, a cysLT1 receptor antagonist, on the enhancement of TNF-α-induced MMP-9 production by cysLTs.

Results ELISA revealed that LTC4 and -D4, but not -E4, enhanced TNF-α-induced MMP-9 production in THP-1 cells and peripheral blood $CD14^+$ monocytes/macrophages. Real-time polymerase chain reaction demonstrated that LTC4 and -D4, but not -E4, increased MMP-9 mRNA expression induced by TNF-α in THP-1 cells. Moreover, we demonstrated that pranlukast completely inhibited the enhancement of TNF-α-induced MMP-9 production by LTC4 and -D4 in THP-1 cells and peripheral blood $CD14^+$ monocytes/macrophages.

Conclusion LTC4 and -D4 enhanced the TNF-α-induced MMP-9 production via binding the cysLT1 receptor in human monocytes/macrophages. Pranlukast inhibited the enhancements by LTC4 and D4.

Correspondence:
Takashi Ichiyama, Department of Pediatrics, Yamaguchi University School of Medicine, 1-1-1 Minamikogushi, Ube, Yamaguchi 755-8505, Japan.
E-mail: ichiyama@yamaguchi-u.ac.jp

Keywords cysteinyl leukotrienes, matrix metalloproteinase-9, monocytes/macrophages, pranlukast, remodelling
Submitted 4 August 2006; revised 14 January 2007; accepted 8 February 2007

Introduction

Matrix metalloproteinases (MMPs) constitute a family of enzymes that mediate the degradation of extracellular matrix proteins [1]. MMPs play important roles in normal and pathological processes, including embryogenesis, wound healing, inflammation, cardiovascular diseases, pulmonary diseases and cancer [2]. MMP-9 is a member of this family, and is capable of degrading collagen IV, a major component of the basement membrane of airways [3]. The activity of MMPs is further controlled by specific tissue inhibitors of metalloproteinases (TIMPs) [4]. TIMP-1 has a high avidity for MMP-9 [5]. The MMP-9, TIMP-1 and MMP-9/TIMP-1 balance is understood to be related to airway remodelling [6, 7]. A recent study demonstrated that allergen-challenged MMP-9-deficient mice had less peribronchial fibrosis and total lung collagen compared with allergen-challenged wild-type mice [8].

Cysteinyl leukotrienes (cysLTs), such as leukotriene C4 (LTC4), -D4 and -E4, induce contraction of the tracheal muscle and have potent effects on leucocyte trafficking, airway mucus secretion and collagen synthesis [9–12]. Normal peripheral blood leucocytes, such as basophils, eosinophils, B lymphocytes and monocytes/macrophages, have a cysLT1 receptor [13]. However, the function of these cells, especially monocytes/macrophages, is poorly understood.

Alveolar macrophages (AM) are the most abundant cells, not only in the alveoli and distal air spaces but also in the conducting airways [14]. Activated AM in asthma may participate in the inflammatory events associated with allergic disease of the lower airways, including the

release of cytokines, chemokines, arachidonic acid metabolites, products of activated O_2 and by direct interaction with T lymphocytes [15–19].

We examined the effect of cysLTs on the productions of MMP-9 and TIMP-1, and on MMP-9 release by previously reported inducers of MMP-9, including IL-13, IL-17, TGF-β1, TNF-α and lipopolysaccharide (LPS), in human monocytes/macrophages [20–24].

Methods

Cell culture and stimulation conditions

THP-1 cells, a human monocytic leukaemia cell line that has a cysLT1 receptor [25], obtained from the American Type Culture Collection, were maintained at 37 °C under humidified 5% CO_2 as stationary cultures. The cells were grown in RPMI 1640 medium containing 10% fetal bovine serum (FBS), 100 U/mL of penicillin and 100 μg/mL of streptomycin. Peripheral blood mononuclear cells (PBMC) were obtained from heparinized blood from 10 healthy medication-free volunteers, with informed consent, by Histopaque 1077 (Sigma Chemical Co., St Louis, MO, USA) gradient centrifugation and washing. Purification of individual cell subpopulations was achieved with a high magnetic gradient Mini MACS purification system (Miltenyi, Sunnyvale, CA, USA). $CD14^+$ monocytes/macrophages were isolated by depletion of non-monocytes (negative selection) with a Monocyte Isolation Kit II (Miltenyi). The purity of the isolated cells was determined using the respective fluorescein isothiocyanate (FITC)-conjugated monoclonal antibodies (Becton-Dickinson Biosciences, San Diego, CA, USA) and flow cytometric analysis (FACScan; Becton-Dickinson Biosciences).

Cells were exposed to 5 ng/mL of IL-13, 5 ng/mL of IL-17, 10 ng/mL of TGF-β1, 20 ng/mL of TNF-α and 1 ng/mL of LPS (from *Escherichia coli*, 0111:B4) and/or cysLTs (Sigma Chemical Company). The doses were determined in accordance with previous studies that investigated MMP-9-relaease by each mediator [20–24]. Some samples were pretreated with pranlukast, a cysLT1 receptor antagonist, provided by ONO Pharmaceutical Co. (Osaka, Japan) for 30 min before the addition of cysLTs. The supernatant fluid, both before and after the addition of cysLTs, was harvested for the determination of MMP-9 and TIMP-1 levels, and then stored at −20 °C.

Determination of MMP-9 and TIMP-1 concentrations

The concentrations of MMP-9 and TIMP-1 were determined with sandwich-type ELISA kits (Amersham, Buckinghamshire, UK). Assays were performed following the instructions of the manufacturer. The detection limits were 0.125 ng/mL for MMP-9 and 2.4 ng/mL for TIMP-1. The assay of MMP-9 recognizes the pro and active forms of MMP-9.

Real-time reverse transcription polymerase chain reaction

Real-time reverse transcription (RT)-polymerase chain reaction (PCR) was performed to determine the mRNA levels of MMP-9 in the THP-1 cells subjected to the indicated treatments. Total cellular RNA was isolated using the TRIzol reagent (Invitrogen, Leek, the Netherlands) according to the manufacturer's instructions. RT was carried out with 2 μg of total RNA and Random Primers (Invitrogen) in a reaction volume of 20 μL using the SuperScript™ III RTS First-strand Strips System (Invitrogen) following the instructions provided. Real-time PCR was carried out using TaqMan Gene Expression Assays and the ABI PRISM 7900 HT Sequence Detection System (Applied Biosystems, Foster City, CA, USA). The PCRs were recorded in real time and analyzed using the accompanying software, Relative Quantification Program. The mRNA level of the GAPDH housekeeping gene was also determined by real-time RT-PCR in each cDNA sample to normalize the expression of the genes of interest (MMP-9).

Statistical analysis

The values of MMP-9 and TIMP-1 concentrations are expressed as means ± SD. Statistical analysis was performed with the Wilcoxon matched-paired test, with a P-value of < 0.05 considered to be significant.

Results

Figure 1 demonstrates total MMP-9 release by the stimulation of LTC4, IL-13, IL-17, TGF-β1, TNF-α and LPS for 24 h in THP-1 cells. Only TNF-α and LPS induced MMP-9 in THP-1 cells. LTC4 significantly enhanced the MMP-9 production induced by IL-13, IL-17, TGF-β1 and TNF-α, but not by LPS (Fig. 1). The enhancement of TNF-α-induced MMP-9 release by LTC4 was significantly greater than that of IL-13, IL-17 and TGF-β1 ($P < 0.01$ for all). The levels of active MMP-9 were lower than the detection limit in the media of cells treated with any stimulators.

LTC4 and -D4 but not -E4 (10–1000 ng/mL) significantly increased MMP-9 release by TNF-α in THP-1 cells, and the potencies of LTC4 and -D4 for TNF-α-induced MMP-9 production were similar (Fig. 2). The potencies of LTC4 and -D4 were not dose related.

The time course of MMP-9 production was examined by incubating THP-1 cells with TNF-α and 100 ng/mL LTC4 during a 48-h period (Fig. 3). MMP-9 production could be observed 8 h after the addition of TNF-α and LTC4, and gradually increased over 48 h.

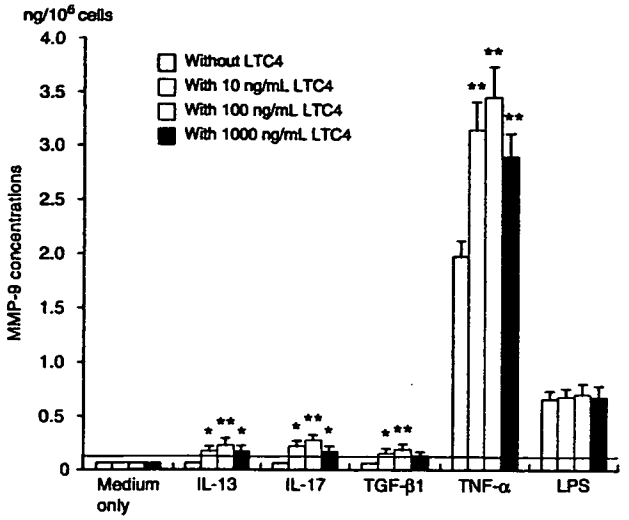

Fig. 1. Matrix metalloproteinase-9 (MMP-9) production, as measured by ELISA, in THP-1 cells stimulated by IL-13, IL-17, TGF-β1, TNF-α or lipopolysaccharide (LPS) with/without LTC4, for 24 h. Data ($n = 8$) are presented as means ± SD. A line indicates the detection limit. $^{**}P < 0.01$ and $^{*}P < 0.05$ compared with cells treated without LTC4.

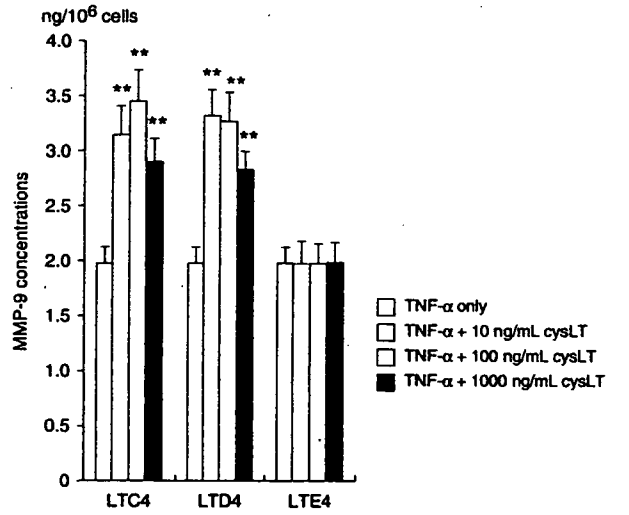

Fig. 2. Matrix metalloproteinase-9 (MMP-9) production, as measured by ELISA, in THP-1 cells stimulated with TNF-α and cysteinyl leukotriene 1 (cysLTs) (LTC4, -D4 or -E4) for 24 h. Data ($n = 8$) are presented as means ± SD. $^{**}P < 0.01$ compared with cells treated with TNF-α only.

ELISA demonstrated that LTC4, IL-13, IL-17, TGF-β1, TNF-α or LPS did not induce TIMP-1 in THP-1 cells (Fig. 4).

The time courses of the inhibitory effects of pretreatments with 10^{-7} M pranlukast on MMP-9 production induced by TNF-α and 100 ng/mL LTC4 were examined in THP-1 cells over 48 h (Fig. 3). Pranlukast blocked MMP-9 production during the experiment. Pranlukast similarly blocked MMP-9 production induced by TNF-α and 100 ng/mL LTD4 during the experiment (data not shown).

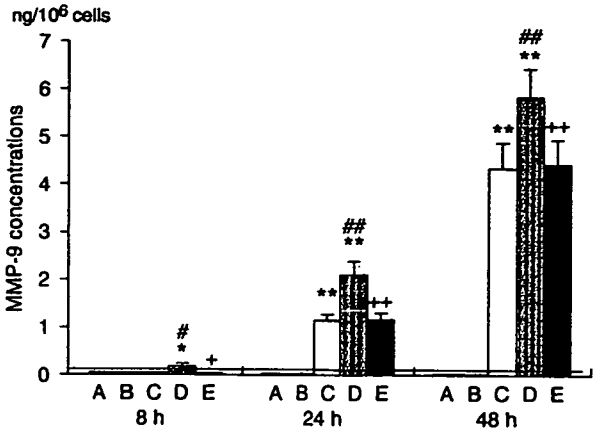

Fig. 3. Kinetics of matrix metalloproteinase-9 (MMP-9) production and the inhibitory effect of pranlukast on MMP-9 release, as measured by ELISA, in THP-1 cells stimulated with LTC4 (B), TNF-α (C) and TNF-α+LTC4 (D) for 8, 24 and 48 h, and cells pretreated with pranlukast for 30 min before TNF-α+LTC4 treatment (E). (A) Cells with no treatment. Data ($n = 8$) are presented as means ± SD. A line indicates the detection limit. $^{**}P < 0.01$ and $^{*}P < 0.05$ compared with cells with no treatment. $^{\#\#}P < 0.01$ and $^{\#}P < 0.05$, compared with cells treated with TNF-α only. $^{++}P < 0.01$, and $^{+}P < 0.05$ compared with cells treated with TNF-α and LTC4.

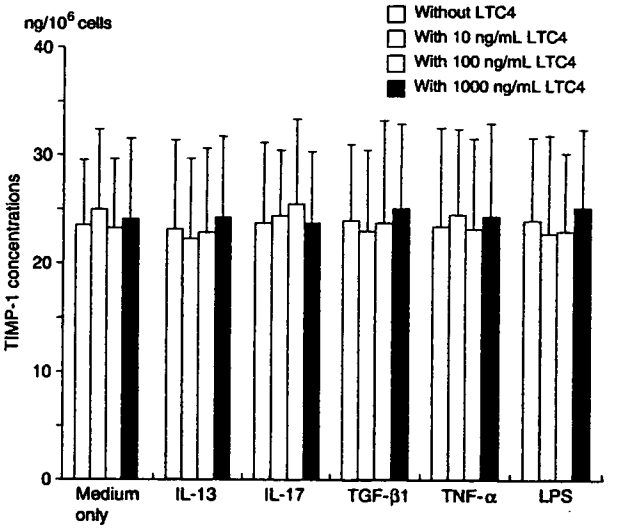

Fig. 4. Tissue inhibitors of metalloproteinases (TIMP)-1 production, as measured by ELISA, in THP-1 cells stimulated by IL-13, IL-17, TGF-β1, TNF-α or lipopolysaccharide (LPS) with/without LTC4, for 24 h. Data ($n = 8$) are presented as means ± SD.

The concentrations of MMP-9 in the culture fluid of THP-1 cells exposed to TNF-α and 100 ng/mL LTC4, -D4 or -E4, in the presence or absence of pranlukast, for 24 h are shown in Fig. 5. The production of MMP-9 induced by TNF-α and cysLTs was significantly inhibited by 10^{-6}–10^{-8} M pranlukast. The effect of pranlukast was dose related.

Real-time PCR demonstrated that MMP-9 mRNA expression was significantly increased 24 h after the

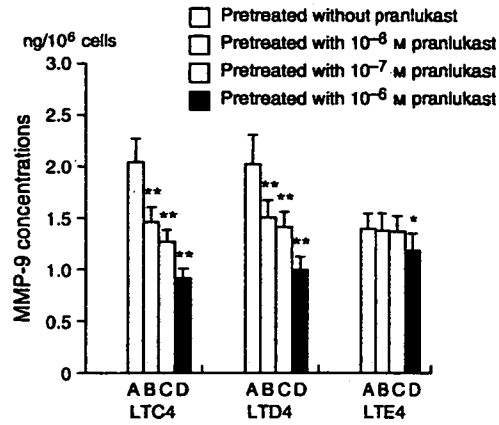

Fig. 5. Inhibitory effect of pranlukast on matrix metalloproteinase-9 (MMP-9) release, as measured by ELISA, in THP-1 cells stimulated with TNF-α and LTC4, -D4 or -E4 for 24 h. The cells were pretreated with pranlukast for 30 min before TNF-α and LTC4, -D4 or -E4 treatments. Cells pretreated without pranlukast (A) Cells pretreated with 10^{-8} (B), 10^{-7} (C) or 10^{-6} M (D) pranlukast. Data ($n = 8$) are presented as means ± SD. $^{**}P < 0.01$ and $^{*}P < 0.05$ compared with cells pretreated without pranlukast.

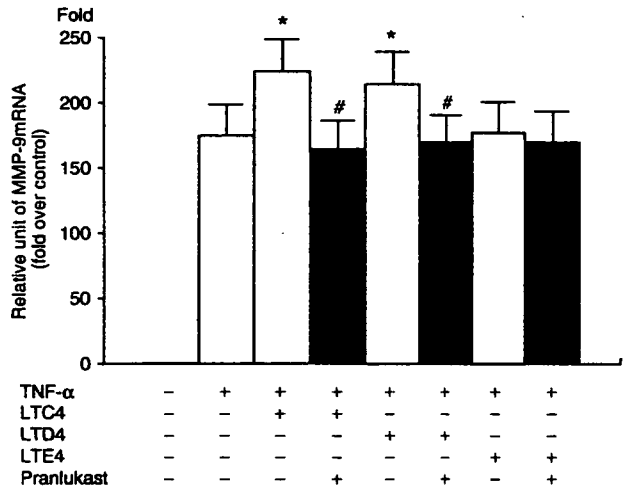

Fig. 6. Matrix metalloproteinase-9 (MMP-9) mRNA expression and the inhibitory effect of pranlukast on MMP-9 mRNA expression, as measured by real-time PCR, in THP-1 cells stimulated with TNF-α and 10^{-6} M LTC4, -D4 or -E4 for 24 h, and cells pretreated with 10^{-7} M pranlukast for 30 min before TNF-α and LTC4, -D4 or -E4 treatments. Data ($n = 8$) are presented as means ± SD. $^{*}P < 0.05$ compared with cells treated with TNF-α only. $^{\#}P < 0.05$ compared with cells treated with TNF-α and LTC4 or -D4.

addition of TNF-α in THP-1 cells ($P < 0.01$) (Fig. 6). Moreover, 100 ng/mL LTC4 and -D4, but not -E4, significantly enhanced the MMP-9 mRNA expression induced by TNF-α (Fig. 6). Pretreatment with 10^{-7} M pranlukast significantly decreased the MMP-9 mRNA expression caused by the stimulation of TNF-α and LTC4, or -D4 in THP-1 cells (Fig. 6).

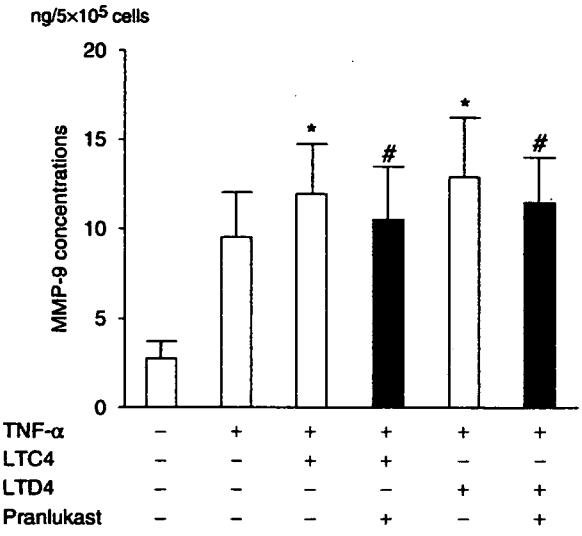

Fig. 7. Inhibitory effect of pranlukast on matrix metalloproteinase-9 (MMP-9) release, as measured by ELISA, in peripheral blood $CD14^+$ monocytes/macrophages stimulated with TNF-α and LTC4 or -D4 for 24 h. The cells were pretreated with pranlukast for 30 min before TNF-α and LTC4 or -D4 treatments. Data ($n = 10$) are presented as means ± SD. $^{*}P < 0.05$ compared with cells treated with TNF-α only. $^{\#}P < 0.05$ compared with cells treated with TNF-α and LTC4 or -D4.

The purity of the $CD14^+$ cells obtained after negative selection with the MACS system was 85.8 ± 6.1%. The MMP-9 production and the inhibitory effect of pranlukast on MMP-9 production were examined by incubating peripheral blood $CD14^+$ monocytes/macrophages with TNF-α and LTC4 or -D4 for 24 h, with some samples being pretreated with 10^{-7} M pranlukast (Fig. 7). LTC4 and -D4 significantly enhanced the MMP-9 production induced by TNF-α in peripheral blood $CD14^+$ monocytes/macrophages ($P < 0.05$). The production of MMP-9 induced by TNF-α and LTC4 or -D4 was significantly inhibited by 10^{-7} M pranlukast ($P < 0.05$).

Discussion

Airway remodelling is an important factor in the pathogenesis of bronchial asthma. MMP-9 is thought to be an important mediator in the airway remodelling of asthma [6, 7, 26–29]. The expressions of MMP-9 in the sputum [26, 30], bronchoalveolar lavage fluid [31] and airway epithelial cells [29, 32] were increased in asthma. In addition, ovalbumin (OVA)-challenged MMP-9-deficient mice have reduced levels of peribronchial fibrosis compared with OVA-challenged wild-type mice [28]. Moreover, MMP-9 induces T cells, neutrophils and eosinophils through the basement membrane [33–35]. It is likely that MMP-9 promotes airway remodelling and inflammation in asthma.

Several recent papers have demonstrated that TNF-α plays a critical role in the initiation and amplification of airway inflammation in asthmatic patients [36–39]. TNF-α induces the adhesion, migration and activation of inflammatory cells, secretion of mucin, apoptosis and the modulation of repair of airway epithelial cells, increased responsiveness of smooth-muscle cells to contractile agents, proliferation and activation of myofibroblasts and fibroblasts and increased synthesis of extracellular matrix glycoproteins [36]. The expression of TNF-α in the airway was related to the severity of asthma [38]. The soluble TNF-α receptor etanercept was beneficial in patients with refractory asthma [39].

Our present study demonstrated that only cysLTs could not increase the expression of MMP-9 in THP-1 cells, but LTC4 and -D4 could enhance TNF-α-induced MMP-9 expression. It is likely that LTC4 and -D4 exert an enhancement of MMP-9 expression induced by TNF-α via the cysLT1 receptor because pranlukast completely blocked the enhancement of TNF-α-induced MMP-9 expression by LTC4 and -D4. The potency of LTC4 and -D4 for TNF-α-induced MMP-9 expression was not dose related. The whole MMP-9 detected in our experiment was the pro form because the levels of active MMP-9 were lower than the detection limit in the media of cells treated with TNF-α in the presence or absence of cysLTs. Ménard and Bissonnette reported that macrophage inflammatory protein-1α (MIP-1α) production induced by 10^{-11} M LTD4 in AM was more than that induced by 10^{-6}, 10^{-8}, 10^{-10}, 10^{-12} or 10^{-14} M LTD4 [14]. We previously reported that monocyte chemoattractant protein-1 (MCP-1) production by cysLTs in human monocytes/macrophages was not dose related [40]. Therefore, it is unlikely that the potency of cysLTs is dose related. Another hypothesis is that higher dosages of LTC4-and -D4 decreased the secretion of MMP-9 because of the potential cell toxicity of LTC4 and -D4 for THP-1 cells. LTD4 would be expected to be about 10 times more potent for calcium flux at the cysLT1 receptors than LTC4 (and 100 times more than LTE4) [41, 42]. The mechanism of enhancement of TNF-α-induced MMP-9 production via cysLT1 receptors of monocytes/macrophages stimulated by cysLTs is different from that of the contraction via cysLT1 receptors of airway smooth muscle stimulated by cysLTs. The potencies of LTC4 and -D4 for the enhancement of TNF-α-induced MMP-9 production in monocytes/macrophages may be different from those for the contraction of airway smooth muscle via the calcium flux.

Pranlukast has some actions in asthma other than as an antagonist of the cysLT1 receptor, including immunomodulation [43]. We have previously demonstrated that pranlukast inhibits the TNF-α-induced nuclear factor-κB (NF-κB) activation [44], and cysLTs-induced MCP-1 production in monocytes/macrophages [40]. In adults administered a single oral dose of 225 mg, Cmax was 642.3 ± 151.0 ng/mL (1.31 ± 0.31 μM) [45], but this value included pranlukast bound to plasma protein. The concentration of free pranlukast was probably less than a tenth of this [46]. Therefore, we think that 10^{-7} and 10^{-8} M pranlukast are clinical doses, and 10^{-6} M is a pharmacological dose. In the animal model, cysLTs promoted airway remodelling in asthma, and the cysLT receptor antagonists inhibited it [10]; however, the mechanism has remained unclear. We revealed one of the mechanisms of airway remodelling associated with cysLTs, and the inhibitory effect of pranlukast. However, the contribution of the anti-remodelling activity of pranlukast at oral therapeutic doses in asthmatic patients remains unclear.

In conclusion, cysLTs enhance TNF-α-induced MMP-9 expression via binding cysLT1 receptor in human monocytes/macrophages *in vitro*, and pranlukast inhibits the enhancement of TNF-α-induced MMP-9 production by cysLTs in the cells.

Acknowledgements

This study was supported by grants from the Ministry of Education, Culture, Sports, Science and Technology (C-17591092), Japan.

References

1 Chandler S, Miller KM, Clements JM *et al.* Matrix metalloproteinases, tumor necrosis factor and multiple sclerosis: an overview. *J Neuroimmunol* 1997; 72:155–61.
2 Chakraborti S, Mandal M, Das S, Mandal A, Chakraborti T. Regulation of matrix metalloproteinases: an overview. *Mol Cell Biochem* 2003; 253:269–85.
3 Nagase H. Activation mechanisms of matrix metalloproteinases. *Biol Chem* 1997; 378:151–60.
4 Murphy G, Knäuper V. Relating matrix metalloproteinase structure to function: why the 'hemopexin' domain? *Matrix Biol* 1997; 15:511–8.
5 Lacraz S, Nicod LP, Chicheportiche R, Welgus HG, Dayer JM. IL-10 inhibits metalloproteinase and stimulates TIMP-1 production in human mononuclear phagocytes. *J Clin Invest* 1995; 96: 2304–10.
6 Atkinson JJ, Senior RM. Matrix metalloproteinase-9 in lung remodeling. *Am J Respir Cell Mol Biol* 2003; 28:12–24.
7 Kelly EA, Jarjour NN. Role of matrix metalloproteinases in asthma. *Curr Opin Pulm Med* 2003; 9:28–33.
8 Lim DH, Cho JY, Miller M, McElwain K, McElwain S, Broide DH. Reduced peribronchial fibrosis in allergen-challenged MMP-9-deficient mice. *Am J Physiol Lung Cell Mol Physiol* 2006; 291:L265–71.
9 Nakai H, Konno M, Kosuge S *et al.* New potent antagonists of leukotrienes C4 and D4. Synthesis and structure-activity relationships. *J Med Chem* 1988; 31:84–91.
10 Henderson WR Jr, Tang LO, Chu SJ *et al.* A role for cysteinyl leukotrienes in airway remodeling in a mouse asthma model. *Am J Respir Crit Care Med* 2002; 165:108–16.

